Supplementary Materials for

Global Patterns of Groundwater Table Depth

Y. Fan,* H. Li, G. Miguez-Macho

*To whom correspondence should be addressed. E-mail: yingfan@rci.rutgers.edu

Published 22 February 2013, *Science* **339**, 940 (2013)
DOI: 10.1126/science.1229881

This PDF file includes:

Supplementary Materials for

Global Patterns of Groundwater Table Depth

Y. Fan, H. Li, and G. Miguez-Macho

correspondence to: yingfan@rci.rutgers.edu

This PDF file includes:

Supplementary Text

S1. Compiling Water Table Observations

S1.1. North America

The United States US Geological Survey (USGS) maintains a national archive on the water data it collects for the nation (http://waterdata.usgs.gov/nwis). Water table observations at 567,946 sites were compiled from the entire archive over 1927-2009. We limit our selection to shallow wells (<100m) to include only unconfined aquifers that are hydraulically linked to the land surface; the aquifer-type code flagged some but not all confined or mixed-confined aquifers, forcing us to adopt a cutoff. Many sites are affected by pumping; time series reveal long-term water level decline. An example is the US High Plains (*35*) where irrigation pumping has lowered the water table by tens of meters (Fig. S1). Pumping also affected other parts of the nation (http://pubs.usgs.gov/fs/fs-103-03/#pdf). About 81% of the sites have only one reading. No efforts are made to compile observations from published literature in the US.

The Natural Resources Canada has recently established a national groundwater information network (GIN) allowing dynamic access to the well information hosted by 8 provinces (http://www.gw-info.net/). Large datasets can also be obtained through the province-level archives at the Waterwell Databases (http://ngwd-bdnes.cits.nrcan.gc.ca/service/api_ngwds:gin/en/downloadmanager/dataset.html?package=waterwells), where we obtained the water level data for 6 provinces (Alberta, Menitoba, Ontario, Quebec, Saskatchewan, and Yukon; Nova Scotia file is empty). Data for Nova Scotia is obtained from the province Well Logs Database (http://www.gov.ns.ca/nse/groundwater/welldatabase.asp). Data for British Columbia was obtained by email request since many wells on the GIN lack water level data (http://ngwd-bdnes.cits.nrcan.gc.ca/service/api_ngwds:gin/en/wmc/aquifermap.html); the Ministry of Environment of British Columbia operates a network of 163 observation wells (http://www.env.gov.bc.ca/wsd/data_searches/obswell/index.html); we received the entire dataset of which 61 wells are in shallow aquifers. The large amount of data (more than US) allows us to choose the shallow wells only. We retained wells <50 m deep, resulting in 163,498 wells from Alberta, 61 from British Columbia, 60,119 from Manitoba, 51,472 from Nova Scotia, 404,124 from Ontario, 66,241 from Quebec, 92,291 from Saskatchewan, and 250 from Yukon, totaling 837,956 site observations over Canada. Except for British Columbia where time series are available, the water table depth retained here is the reported static water level found in a well when it is first completed; i.e., the many wells reflect conditions at different times.

A total of 1,405,902 site observations are compiled from North America.

S1.2. Western Europe

The French ADES Groundwater National Portal provides a freely accessible groundwater level and quality information (http://www.ades.eaufrance.fr/) at thousands of wells. Time series of water levels at >3,000 wells, organized into 22 regions, were downloaded. After excluding artisan wells (head higher than land surface elevation) and deep wells (>100 m deep), 2,837 wells were left and the mean water table depth at each well is obtained.

Groundwater data in Germany is maintained by the state geologic surveys (http://www.bgr.de/geol_la/geol_la.htm). According to BGR, the Federal Institute for Geosciences and Natural Resources, 70% of drinking water in Germany comes from the groundwater (http://www.bgr.bund.de/EN/Themen/Wasser/wasser_node_en.html). In Bavaria, the State Office of Environment offers free access to daily, weekly and long-term statistics of groundwater level at 218

wells in shallow and 65 wells in deep aquifers (http://www.nid.bayern.de/grundwasser/index.php?thema=niedrigwasser&days=0&wert=grundwasser). Excluding the wells in bedrocks from the upper aquifers resulted in 182 wells. The mean water table over a record period of 2-97 years (depending on sites) is downloaded. In Hessen, weekly observations of water level at 61 monitoring wells (only over the past 14 months) can be downloaded from Hessisches Landesamt of Environment and Geology (http://www.hlug.de/start/wasser/grundwasser/grundwasserstaende-und-quellschuettungen.html), of which 30 are in unconfined surficial aquifers. Groundwater withdraw may have influenced the observed levels because the majority of the state's drinking water comes from the groundwater. In Mecklenburg-Vorpommern, the state Geological Survey has an interactive map showing the wells (http://www.lung.mv-regierung.de/insite/cms/umwelt/geologie/fis_geo/landesbohrdatenspeicher.htm). Clicking each well symbol displays the location, land elevation, well depth, and water table head at the beginning and ending of the record period which ranged from one single reading to several decades. Without the entire record or long-term statistics, we calculated the mean of the two readings. Where multiple wells at different depths are given a single location, the shallowest well is chosen. A total of 293 site observations are obtained this way. In North Rhine-Westphalia, the State Office for Nature and Environment maintains a comprehensive web dataset (http://www.elwasims.nrw.de/ims/ELWAS-IMS/viewer.htm) with >52,000 groundwater monitoring sites. By clicking each site, well information (location, depth, aquifer type) is displayed and long-term time series of summer and winter water levels can be downloaded as excel files. Because of the large number of wells, we requested the entire dataset which was graciously sent to us in its entirety. After removing sites with missing water level, location and well depth, and after removing wells deeper than 50m (to emphasize shallow aquifers, affordable due to the large number of wells) we retained 28,386 sites with record length of at least 1yr, which ranged from 1-107yr with a mean record length of 25yrs. In Saxony, the state Agency for Environment and Geology maintains a website holding all geospatial data of the state including groundwater measurements at over 1,300 wells of its dense monitoring network (http://www.umwelt.sachsen.de/umwelt/infosysteme/weboffice/synserver?project=wasser&language=de&view=gwm). Recent and long-term (multi decades) water level readings can be downloaded by selecting polygons. We obtained the mean water table depth at 655 monitoring wells. In Saxony-Anhalt, the state Agency for Flood Protection and Water Management (LHW) publishes reports of surface and groundwater monitoring results (www.lagb.sachsen-anhalt.de/). Reports for 2008 and 2009 are available from which 301 shallow monitoring wells (<50m deep) have water level readings (1 to 6 times). In Schleswig-Holstein, the state Agricultural and Environmental Atlas displays over 1000 groundwater level and quality monitoring wells (http://www.umweltdaten.landsh.de/atlas/script/index.php). By clicking each well, the latest 100 water level measurements are displayed. Because of the high density of wells, we chose only those that are <50m deep to better reflect the phreatic aquifer conditions, and if there are multiple wells at different depth at each site, the shallowest (coded F1) is chosen. The mean water levels at a total of 397 wells are obtained. A total of 30,244 site observations are compiled from the above 7 state governments. Data was not found for other states because they either do not have an open data portal, or charge a fee to send us the data that we do not have funding for, or did not respond to our email requests.

In the Netherlands, the Dutch Institute of Applied Geoscience (TNO-NITG) maintains a national database on groundwater at tens of thousands of wells (DINO, http://www.dinoloket.nl/en/DINOLoket.html) free for non-commercial use. The well data, organized into 6 regions, are downloaded and the mean of each time series is obtained at 43,399

sites, the entire DINO database. The Netherlands have the densest water table observations of all nations. Widespread groundwater pumping for water supply and land drainage throughout the centuries has been well documented (*36*).

In the Iberian Peninsula (Portugal and Spain), data were obtained from the Instituto Geológico y Minero de España (IGME, Institute of Geology and Mining of Spain) and from the Portuguese Sistema Nacional de Informação de Recursos Hídricos (SNIRH, National Information System for Hydrological Resources, http://snirh.pt/index.php?idMain=). Both nations have a state-owned groundwater monitoring network. Additional data for Spain were compiled from several Confederaciones Hydrográficas (rivers Ebro, Duero, Tajo, and Júcar), agencies managing the main watersheds within the country. Most records in the dataset consist of measurements reported at irregular time intervals, in general once per month or at least several per year, for a time span of a few years. Discarding locations with well depths of more than 100 m to eliminate measurements in confined aquifers, we have a total number of 2,601 observation points. We only retained points with temporal records longer than 4 years (2,085 in total). Water table decline due to pumping is apparent in the south of the northern plateau region (Castile and León, Spain), and it is even more acute in La Mancha and the province of Alicante in eastern Spain. There are problematic sites spread out elsewhere, especially in the South. In a Mediterranean climate, the growing season coincides with the dry season, so pumping for irrigation occurs even in wet years. We eliminated sites with declining trends of > 0.6 m per year. The number of points eliminated in this manner is 445, leaving 1,640 sites.

A total of 78,180 site observations were compiled from Western Europe.

S1.3. Australia

Groundwater monitoring and data archiving are administered by the individual territories. Some of them make the data free to the public via web-download or a formal request, and others charge a fee for data processing. The territory of New South Wales maintains a groundwater database (http://www.waterinfo.nsw.gov.au/) of 126,900 wells. We obtained the entire record with a processing charge of $220. Only wells <100m deep, with complete latitude and longitude information are retained, giving a total of 26,857 wells. Our data request to Northern Territory was not answered, but borehole logs are free to the public from the interactive map site of NRETA (http://www.nt.gov.au/nreta/water/ground/index.html). By clicking each individual bore on the map, the location, well depth and water level are recorded. But water level is missing at most of the many thousands of wells, particularly the shallow wells that are desirable for our purpose. In addition, a value of zero was entered where the water level is missing, hence excluding the wells where the water level is indeed at the land surface. Large and dense clusters of wells are found over cities, which are avoided because of heavy pumping reported at the wells. Large production and irrigation wells in the rural area are also excluded to minimize pumping influence. Where multiple wells are shown at a single location, the shallowest one is chosen. This labor-intensive effort took several months and yielded a total of 3,274 site observations. Thousands of observation wells are maintained by the Queensland Department of Environment and Resource Management (http://www.derm.qld.gov.au/services_resources/item_details.php?item_id=32731). Our request was granted and we obtained the entire archive of the observation network. After removing wells >100m deep, we retained the mean of multiple readings at 4,292 wells. In South Australia, the OBSWELL program of the Department of Water, Land and Biodiversity Conservations maintains >800 observation wells (no pumping) which can be freely downloaded (https://obswell.pir.sa.gov.au/new/obsWell/MainMenu/menu). After removing deep wells (>100m) and artesian wells (head above land surface), 456 wells are retained. The Victoria State Observation Bore Network (http://www.water.vic.gov.au/monitoring/groundwater) monitors the groundwater

quality at ~2500 wells with the data free to the public. Using "Selection by measurement type" we found 660 of the wells with water level data. Data for each well was downloaded and processed one by one. After removing deep wells (>100m) we obtained 477 time series of water level (6 to 3780 measurements). The entire archive on groundwater wells in Western Australia was downloaded via the Geographic Data Atlas website (http://www.water.wa.gov.au/Tools/Maps+and+atlases/Geographic+data+atlas/default.aspx) maintained by the Department of Water (DoW) Water Information (WIN), totaling 60,878 wells with static water level data. The aquifer type information (http://www.anra.gov.au/topics/water/overview/wa/gmu-perth-superficial.html) allowed us to remove wells not in the "surficial" or "superficial" category, leaving 48,261 wells.

A total of 83,617 well site observations were compiled from Australia.

S1.4. South America

We searched the government database of each country in S. America and each province except for Brazil and Chile which have national archives. To supplement the sparse observations, we searched the published literature. Many articles are found that reported the water table depth. Where data are presented as plots or maps we recorded the approximate values.

In Argentina, groundwater information is collected by water companies associated with provinces or municipalities in different ways with different quality controls. Requests sent to the individual provinces (http://www.hidricosargentina.gov.ar/sitios-organismos.html) were not answered. Searching province websites yielded data from La Pampa, La Rioja, and Mendoza. In La Pampa, WTD time series exist at 73 wells (see http://www.bdh.lapampa.gov.ar/lapampa/well/list.jsp) with 7 showing water level changes >200m in a month, likely caused by pumping in confined aquifers and hence removed. For La Rioja (http://www.larioja.gov.ar/sda/secundarias/perforaciones.html) water levels are found but well location is in descriptive terms such as "4 km al norte de Vinchina sobre banquina der. Ruta a Valle Hermoso" (4 km north of Vinchina on the right side of the road to valle Hermoso). Fifteen publications are found where the observations were not affected by irrigation or pumping (*37-51*).

In Bolivia, no government data was obtained despite repeated requests. One published article reported observations in the Bolivian Amazon (*52*).

The Brazilian Geological Survey is the largest data source with over 33,570 wells in unconfined aquifers (http://siagas.cprm.gov.br/wellshow/indice.asp?w=800). But they are concentrated in the developed east and southeast and clustered over large metro regions (Fig. S2). The wells are drilled for groundwater exploitation; groundwater is considered cleaner and has become a major source for municipal supply. About 95% of the wells in the dataset report high pumping rates. Figure S2 shows the principle aquifers and aquifer systems (color patches) and the metro regions in Amazonia situated on and are supplied by these aquifers. Some of the aquifers in the east have seen regional water table decline of >20m in recent years. Fourteen publications are also found with observations (*23, 25, 53-63*).

In Chile, WTD time series are found for 30 wells by Dirección General de Águas (http://www.dga.cl/index.php?option=content&task=category&sectionid=16&id=43&Itemid=169), plus one publication (*64*).

Repeated requests to Colombia were made. We found one publication with 1 observation (*52*).

In Ecuador, the Instituto Nacional de Meteorología e Hidrología provides an inventory list of 3,589 wells and springs (http://www.inamhi.gov.ec/html/inicio.htm) but actual water level is published only for the Rio Mira basin (146 sites). Observations at 5 sites are reported in a publication (*52*).

The Insituto Nacional de Recursos Naturales of Peru holds pfd reports of hydrogeology investigation (17 reports at http://www.inrena.gob.pe/irh/irh_est_hidrogeologicos.htm, and 29 reports at http://www.inrena.gob.pe/irh/irh_proy_asubterraneas_act.htm) but they do not give information on the location of the thousands of wells, except for the valley of Ica which has a separate inventory report (on bottom of the page: http://www.inrena.gob.pe/irh/irh_proy_asubterraneas.htm) yielding 66 site observations. We emailed and telephoned the contact given on the website and were assured that an expert would get back to us. The report of Iquitos includes a map of the wells, which is gridded into 128 cells of 300m by 300m and the mean in each cell is averaged. The report of Motupe includes a map of cities after which groundwater zones are named and water table range given, yielding 13 points. The same method is used to obtain 16 points from the La Leche report and 2 points from the Pucallpa report. Observations at 21 sites in the Peruvian Amazon are found in two publications (*52*, *65*).

For Suriname, a Ph.D. thesis provided detailed studies of the rainforest climate, geology, hydrology and ecology (*66*).

In Venezuela no government data were obtained despite repeated requests. Two publications are found with study sites in southern Venezuela (*67-68*).

A total of 34,508 site observations were compiled from the continent of S. America.

S1.5. Africa

The Scientists of the French-sponsored research project AMMA (African Monsoon Multidisciplinary Analysis, see http://amma-international.org), Drs. Guillaume Favreau, Yahaya Nazoumou, and Luc Séguis kindly provided us with 197 site observations of water table depth, which was the largest data source we found in Africa. From published literature, we found another 234 site observations from 18 African nations (*69-104*), making a total of 431 data points from Africa.

S1.6. Asia

A lack of open-access government data necessitated a country by country search. An extensive search of published literature resulted in 99 articles with water table reported at 1,143 locations. Widespread groundwater pumping, irrigation and drainage led to many of the published data not useful for our purpose (focusing on natural hydrologic conditions) so hundreds of papers are reviewed but not reported here.

The Bangladesh Water Development Board mains a national network of ~1,255 shallow groundwater monitoring wells with decades of water level data sampled at weekly intervals (http://www.bwdb.gov.bd/), but the data is not freely accessible. Our literature search lead us to two published papers (*105-106*) that applied the dataset to investigating groundwater changes. The authors of the papers, Drs. M. Shamsudduha and R. Taylor graciously sent us the data they had negotiated with the Bangladesh Water Development Board through an agreement. To minimize the influence of groundwater pumping induced water level decline, only the data collected in 1976, the beginning of groundwater monitoring and representing the pre-development period, is selected. This has reduced the number of wells to 234. The yearly mean of weekly observations are used here.

One paper was found in a tropical evergreen forest in the Mekong Basin in Cambodia with one well (*107*).

There exists an extensive literature on groundwater investigations in China, but most focused on regions with large-scale and long-term irrigation, river diversion and groundwater pumping such as the North China Plain and the Tarim Basin. Excluding those or selecting data from pre-development periods when available, we are left with 23 publications (*108-130*) from which we compiled 146 site observations.

The India Central Ground Water Board manages ~15,000 groundwater monitoring wells (http://www.india.gov.in/outerwin.php?id=http://cgwb.gov.in/) with the aid of the World Bank, but the data are not publically available. We searched the literature and found 36 published field studies (*131-166*), from which we obtained 242 well observations. Groundwater pumping and irrigation occur widely in India as reported in the literature, and we attempted to select data that are least affected (e.g., discarding data obviously affected, and using pre-development period).

The Iran Water Resources Management Company (http://www.wrm.ir/) under Ministry of Energy holds a large amount of groundwater information as cited by published literature as the data source, but the site is only available in Persian language. We found a large body of published literature on groundwater conditions but most of the study sites are either heavily irrigated or the groundwater severely depleted. We found nine studies that are focused on the geology in undeveloped regions of Iran or presented data in the 1980s and 1990s before the severe decline was detected (*167-175*). We obtained 102 site observations.

For Kuwait, one paper was found reporting water table depth for 8-10yrs at six wells (*176*).

For Mongolia one paper was found that reported water table depth at one location using ground penetrating radar (*177*).

For Oman, two papers were found reporting water table depth at 30 wells (*178-179*).

For Pakistan, one paper was found with data at 3 sites (*180*). Others did not give well location.

We found eight articles reporting water table depth in Russia (*29*, *181-187*) at 14 sites.

We found four articles (*188-191*) reporting observations at 6 sites Saudi Arabia.

The South Korean National Groundwater Monitoring Stations (NGMS) maintain 320 monitoring wells since 1995, but the data download websites are not available in English. Two papers described the network and analyzed groundwater trends (*192-193*), and we obtained the mean water level at 154 shallow wells from the author Dr. J-Y Lee.

Two papers are found (*194-195*) reporting 4 site observations in Thailand.

Although there exists a large number of groundwater studies in Turkey almost all are over regions with intense irrigation and drainage. Three papers are found in natural settings or with pre-development data (*196-198*) giving 14 site observations.

Two papers are found with detailed investigations in United Arab Emirates (*199-200*). One of them provides a high resolution water table contour map based on a dense seismic survey for oil exploration conducted by the US Geologic Survey. Together 184 site observations are obtained.

Two papers gave 2 site observations on the Mekong Delta, Vietnam (*201-202*).

A total of 1,143 data points are obtained from Asia.

S1.7. Summary

There are also indirect data sources such as mapped perennial wetlands and streams where the water table is at or above the land surface, but they are not used here to avoid biasing the observations toward shallow WTD conditions. We obtained a total of 1,603,781 site observations, 1,405,902 from N. America, 83,617 from Australia, 78,180 from Western Europe, 34,508 from S. America, 1,143 from Asia, and 431 from Africa. Our data compilation is ongoing and the amount of data will grow as more government agencies make their data available online and as we continue to search for published observations.

S1.8. Acknowledgement

We thank the following colleagues for assisting us in compiling the observations. They answered numerous email requests from us and have gone out of their ways to assemble the complete observations (geographic location, well depth, aquifer type, well history, human influence,

and water table time series) and often had to create a download site just for us. This project would have been impossible without them.

US: The scientists and staff at the US Geological Survey for over a century of systematic monitoring of the nation's water resources and for maintaining a state-of-art national database.

Canada: Azina Kanji and Carole Holt Oduro (Alberta Environment), Kei Lo (Saskatchewan Watershed Authority), Bob Betcher and Janie Ulrich (Manitoba Water Stewardship), Dajana Grgic and Christina Girjoaba (Ontario Ministry of the Environment), Fern Schultz, Celine Davis, and Lindsey MacFarlane (British Columbia Ministry of the Environment).

Australia: Aaron Reading (Dept. Environment and Resource Management, Queensland) and Joanne Gregory (Data Management Office, Western Australia).

Germany: Drs. Dirk Pilchowski and Peter Fritsch (Bavarian Environmental Agency), Dr. Wolfgan Wolters (Schleswig-Holstein Ministry of Agriculture and Environment), Dr. Jörg Schubert (Saxony State Office For Environment, Agriculture And Geology), Dr. Dieter Feldhaus (Saxony-Anhalt state Agency for Flood Protection and Water Management (LHW)), Dr. Heinrich Heuser (North Rhine-Westphalia state Geological Survey), Drs. Volker Cremer and Dietmar Wyrwich (North Rhine-Westphalia state Office for Nature and Environment). Dr Wyrwich assembled the entire state dataset (at >37,000 monitoring wells) and created a download site for us.

South America: Dr. Pedro Silva Dias (Universidade de Sao Paulo), Dr. Flavia Nasinmento (Brazilian Geologic Survey), Dr. Victor Donato leandro Silva (Instituto Nacional de Recursos Naturales, Peru), Dr. Luis Mosteiro Ramirez (Programa de Informacion y Documentacion Cientifica y Tecnica del CEDEX, Spain), and Lic. Daniel Cielak (Banco de Datos Hidrologico Subsecretaria de Recursos Hidricos de la Nacion, Argentina).

Asia: Drs. M. Shamsudduha and R. Taylor for sharing the Bangladesh data, Dr. Jin-Yong Lee for sharing the South Korea National Groundwater Monitoring Network dataset, and Mr. Alex Fiore (graduate student at Dept. Earth and Planetary Sciences, Rutgers University) for help in searching the literature for Asia observations.

Africa: The scientists and PIs of AMMA (African Monsoon Multidisciplinary Analysis, see http://amma-international.org) Dr. Guillaume Favreau (IRD, Research Institute for Development, France), Dr. Yahaya Nazoumou (Univ. Abdou Moumouni, Niger), Dr. Luc Séguis (Univ. Montpellier, France), and Dr. Christophe Peueot (IRD, Bénin).

Finally, we thank the many authors of the published literature (reference *23, 25, 27, 35-202*) from which we have obtained observations where they are most needed (lacking government data, or in remote regions of the world). The efforts of those individuals who have toiled in the fields in remote and often unsafe regions of the world are deeply respected and most gratefully acknowledged.

S2. The Groundwater Flow Model

S2.1. Formulation

We evoke hydrologic equilibrium to focus on the spatial patterns resulting from long-term adjustments of water balance to the mean climate, terrain and sea-level forcing (Fig. S3). Climate is expressed in the recharge flux (R), equivalent to soil drainage, obtained from global land models (R=P-ET-Qs, P=annual precipitation, ET=evapotranspiration, Qs=surface runoff). Terrain influence is by gravity-driven groundwater convergence (Q) from high to low elevations per Darcy's law (SM). Along coastlines the water table equates the sea level (hydraulic head boundary condition). Thus the recharge (R) in upland cells sustains lateral divergence (sum of Q in 8 directions), which converges into valley or coastal cells feeding wetlands and rivers (Qr). Thereby climate-induced vertical influx is redistributed laterally by terrain-induced groundwater flow, ultimately constrained by the sea level, and the WTD at any location reflects this recharge-drainage balance.

At the hydrologic equilibrium, mass balance dictates that at a hillslope cell, recharge (R) balances lateral divergence (sum of *Q*) to the lower neighbors (Fig. S3a):

$$R = \sum_{1}^{8} Q \tag{S1}$$

In valley cells, lateral convergence (sum of *Q*) balances discharge into rivers and wetlands (Q_r):

$$\sum_{1}^{8} Q = Q_r \tag{S2}$$

Equation (S2) also applies to coastal cells where groundwater emerges before the sea. River-wetland cells appear naturally in the simulation where water table rises above land surface as determined by mass balance. At these cells, the water table is reset at the land surface at each iteration step, mimicking the removal by surface drainage and evaporation. The lateral groundwater flow between model cells (*Q*) is calculated with the Darcy's Law (*203*), which relates the water table slope to the flow rate:

$$Q = wT\left(\frac{h - h_n}{l}\right) \tag{S3}$$

where *Q* is the flow between the center cell and neighbor n, w the width of cell interface, *T* the transmissivity (explained later), *h* the water table head above sea level, h_n the head in neighbor cell n, and *l* the distance between the center of the two cells. To obtain *T* (integration of hydraulic conductivity over flow depth), we examine two cases (Fig. S3b): water table above or below the depth (d_0) of known hydraulic conductivity (K_0). The distinction is necessary because global soil datasets do not include information beyond ~1 m depth, and the two cases must be treated separately. In Case-a, the water table depth d_1 is above d_0 and we have,

$$T = T_1 + T_2\,, \quad T_1 = K_o\,(d_0 - d_1), \quad T_2 = \int_0^{\infty} K dz' = \int_0^{\infty} K_0 \exp(-\frac{z'}{f}) dz' = K_0\, f \tag{S4}$$

where *z'* is depth below d_0, with *K* assumed to decrease exponentially from K_0 (more later),

$$K = K_0\, exp\,(-z'/f) \tag{S5}$$

where f is the e-folding depth (more later). In Case-b, the water table is d_2 below d_0 and we have,

$$T = \int_{d_2}^{\infty} K dz' = \int_{d_2}^{\infty} K_0 \exp(-\frac{z'}{f}) dz' = K_0 f \exp\left(-\frac{z-h-d_0}{f}\right) \quad \text{(S6)}$$

where z is land surface elevation of the center cell.

S2.2. Hydraulic Conductivity

To calculate groundwater flow, hydraulic conductivity K for the geologic material is needed beyond the top ~1 m of soil. A global permeability dataset has been created (*10*), but due to technical difficulties, we could not adopt it in the present modeling framework. Lacking better alternatives, we rely on a common assumption on its vertical distribution. Continental crustal and sediment permeability generally decreases exponentially with depth at kilometer to decameter scales (*204-206*) because weathering and pressure release initiate at the land surface. In the absence of real aquifer hydraulic parameters, many studies have relied on this general relationship to capture this systematic change in permeability with depth (*205*).

However, the rate of decay, as represented by the parameter f (Eq. S5), cannot be uniform across all geologic settings but should reflect the sediment-bedrock profile at a location. This profile is a complex function of geologic, climate, and biotic history, but the weathering-erosion-sedimentation balance depends strongly on terrain slope (*207*); steep slopes shed and flat valleys accumulate sediments. Climate plays a key role but the mechanisms are more complex; low rainfall produces low erosion leading to sediment accumulation and deep regolith; but high rainfall leads to deep percolation, denser biota, enhancing weathering and resulting in deep regolith as well. For simplicity with the first order control, we consider the terrain slope only.

The f as a function of slope s is determined by calibration to best reproduce water table and wetland observations in N. America (*3*, more discussed under Model Calibration and Evaluation):

$$f = \frac{a}{1+bs}, \quad f > f_{min} \quad \text{(S7)}$$

where a, b, and f_{min} are calibration constants, and s is the terrain slope.

In our earlier work over N. America (*3*), the digital land elevation is the 1 km grid GTOPO over the US, the most accurate dataset for the US obtained by digitizing USGS land survey maps. For the rest of the world, GTOPO has varying degrees of accuracy depending on local data source. For this study, we need a global coverage with consistent accuracy. We use the 30" grid USGS HydroSHEDS from NASA Shuttle Radar Topography Mission (SRTM) and processed for hydrologic studies such as delineating river networks (dams removed, pits filled) (http://hydrosheds.cr.usgs.gov/). Since SRTM does not cover beyond 60°N, topography of higher latitudes is obtained from the NASA-JPL ASTER Global Digital Elevation Map (http://asterweb.jpl.nasa.gov/gdem.asp) at the 1" (~30m) grid averaged to 30" for this study. We did not use the ASTER for the entire globe despite its global coverage because the product exhibits NE-SW stripes (satellite paths, see Fig. S12 and S14, north of 60°N). This composite global elevation dataset is the best for our purpose at the present. Terrain slope (s, in Equ. S7) derived from this dataset, at the 30 arc-second grid, is shown in Fig. S4a.

Equation S7 was developed for the temperate regions of N. America and it leads to a water table that is too deep in cold climate with frozen ground, the latter hydrologically manifested as impeded drainage similar to thin soils over bedrocks. We modify Eq. S7 to include the temperature control on drainage depth. Both seasonal-frost-penetration-depth and permafrost-seasonal-thaw-depth follow the spatial pattern in winter air temperature (*208*). Soil thermal properties (e.g., peat content), geothermal gradient, snow depth and soil water content also influence the freeze-thaw depth, but we maintain simplicity and consider only the first-order control by introducing a two-piece linear temperature modifier, *fT*,

$$fT = 1.5 + 0.1T \qquad (-14\,^{o}C < T < -5\,^{o}C,\ fT<=1)$$

$$fT = 0.17 + 0.005T \ (T < -14\,^{o}C,\ fT>=0.05) \qquad \text{(S8')}$$

where c_1, c_2, c_3 and c_4 are calibration constants (discussed under Model Calibration and Evaluation), *T* is January surface air temperature in ^{o}C (Fig. S4b), -5 ^{o}C corresponds to the approximate southern limit of significant seasonal frost penetration (>0.5 m) (*209*), and -14 ^{o}C corresponds to the approximate southern limit of patchy permafrost associated with peat accumulation in N. America (*208*). The constants are adjusted to best reproduce observed wetland areas in these two thermal regimes (*3*). The final *f* is the product of Eq. S7 and S8. The result (Fig. S4c) is a diminishing soil depth (lower *f*) at steeper slopes and lower temperature, reflecting land slope in warmer but winter temperature in colder climates. Large *f* values represent deeper aquifers, larger flow cross-sectional area (larger conduit), and hence more efficient cell-to-cell groundwater flow. We note that Fig. S4c correlates very well with the sediment thickness (http://igppweb.ucsd.edu/~gabi/sediment.html) in the top 2 km of earth's crust in the warmer parts of the continents, suggesting that our slope-dependent permeability profile captures the first-order physical principle that erosion moves sediments from high-steep slopes to low-flat basins.

S2.3. Soil Hydraulic Parameters

Soil information is derived from UNESCO Food and Agriculture Organization (FAO) digital soil map of the world (http://www.fao.org/nr/land/soils/digital-soil-map-of-the-world/en/) at the 5 arc-minute spacing, replaced in the US with STATSGO (http://soildatamart.nrcs.usda.gov/SDMDB/GSMFULL.htm) from the US Department of Agriculture (USDA) at 30 arc-second grids. Fractions of silt, clay, sand, and organic carbon are used to produce 12 soil-texture classes according to the USDA classification system (http://soils.usda.gov/education/resources/lessons/texture/). Organic soil (peat) is identified as soil organic carbon >12% (*210*). The 12 classes are assigned permeability (K_0 in Eq. S4-S6) with empirical functions (*211*) widely used by the climate and hydrologic modeling communities.

S2.4. Water Table Recharge

The climate forcing is the recharge, *R* in Eq. S1 and Fig. S3a, or the net flux across the water table. Point measurements using tracers or catchment assessments using mass balance or hydrographs are by necessity limited to individual sites. A global assessment of this flux, in a climatologic-mean sense, is best achieved by fully coupled vegetation-soil-groundwater model simulations, forced by observed atmosphere and constrained by field measurements. Figure S5 shows the six global model estimates considered here: Döll-Fielder (*8*) using the WaterGAP Global Hydrology Model WGHM over 1961-1990, forced by two observation-based global precipitation products (CRU and GPCP), Wada-et-al (*212*) using the global hydrology model PCR-GLOBWB over 1958-2000, and by three land hydrology models (CLM, MOSAIC, and NOAH) in the Global

Land Data Assimilation System (GLDAS) over 1979-2008 (*213*). The two Döll-Fielder estimates are nearly identical and the mean is used here. We note that only Döll-Fielder estimates are validated with observed streamflow records (they used >2000 records worldwide). The three GLDAS estimates, although with identical forcing, differ greatly from one another. We evaluated all of the recharge estimates over N. America where observations are most abundant. Döll-Fielder GLDAS-CLM3 gave the results that best reproduced the observed water table depth and wetland extents in N. America (details later), and hence are used for subsequent analyses and discussions.

The sensitivity of the simulated WTD to the choice of recharge was investigated in detail in N. America where the three GLDAS estimates are applied (*3*) and in S. America with an additional estimate from ECMWF land model HTESSEL (*214*). The results show relatively low impact on the simulated water table. The low sensitivity to recharge is due to the well-known self-limiting groundwater drainage process (*215-218*); as recharge increases, the water table rises, steepening the hill-to-valley hydraulic gradient, and expanding the channel network through groundwater seepage, both accelerating drainage and bringing down the water table; as the recharge decreases, the water table falls, flattening the hydraulic gradient and lowering the water table below stream beds, both reducing discharge and preserving groundwater stores. This negative feedback dampens the water table sensitivity to recharge uncertainties.

We note that the recharge estimates considered here are likely biased high in the arid, internal-drainage basins where lateral river and groundwater convergence to the valleys supports high evapotranspiration rates leading to the formation of salt lakes and playas. That is, recharge on the arid valley floors is in reality negative (net loss to the soil and atmosphere above). For example, evaporation from the floor of Pilot Valley near the Nevada-Utah border in the US was estimated to be ~1,380 mm/yr based on multiple field methods (*219*); given that precipitation is ~80 mm/yr (*220*), the recharge is -1,300 mm/yr. However, without lateral convergence in these global models used to obtain recharge here, such high ET is not possible because it is limited by local rainfall. Without the large negative recharge here, our model must allow the water table to rise to the land surface to be removed (recall that it is reset to land surface at each iteration step, mimicking surface water drainage and evaporation). The recharge bias will no doubt lead to a simulated water table that is too shallow in the arid valley floors. We note that Döll-Fielder recharge is significantly lower than CLM recharge in the arid parts of the world, and we expect that it will perform better in these regions.

S3. Model Evaluation

Figure S6 gives a visual comparison between the observed and simulated water table depth (WTD) in Western Europe at the grid cells with observations. Western Europe is shown because of its dense and long-term records, and the wide range of observed WTD. The deeper observed water table in Spain and France is at least partially caused by pumping that is absent in the model. The WTD in the more humid areas (Netherlands and Germany) agrees well between observations and the model. Statistical evaluation is presented later.

S3.1. Calibration Using Observations from Temperate N. America

The parameter f (in Eq. S5, the e-folding length of exponential decrease of hydraulic conductivity with depth) is calibrated to empirically constrain the constants in Eq. S7 and S8. The functional forms are as simple as possible (minimum parameters) that give the desired properties (nonlinear, negative slope) while the constants are obtained from multiple simulations to minimize the residual (model-observation).

Earlier we calibrated Eq. 7S over temperate N. America (lower 48 states) at the grid resolution of 1.25 km using 549,616 site observations compiled up to then (*221*). Tens of simulations were performed to produce the target residual distribution by manually adjusting *a* and *b* in Eq. 7S. The result was,

$$f = \frac{120}{1+150s}, \quad f>5\text{m} \qquad \text{(grid = 1.25km)} \qquad \text{(S7')}$$

That is, at completely flat cells (s=0), the e-folding depth is 120 m, at which the hydraulic conductivity K is reduced to *1/e* or 37% of the surface value, a very deep sediment profile indeed as commonly observed in large sedimentary basins and coastal plains.

However the constants in Eq. S7 depend on model grid resolution. As grid size decreases, local topography is better resolved, the apparent land slope is steeper, and drainage is accelerated, resulting in a deeper water table under high grounds. The grid size of 1.25 km used to derive Eq. S7' above is chosen because the goal of that study was to couple the water table dynamics to a specific regional climate model (RAMS) configuration, with a common land grid of 12.5 km over N. America in the polar-stereographic projection. The 1.25 km grid for the water table simulation there divide each land grid cell into 10x10 subgrid cells to capture the local features in WTD.

Because of their scale-dependence, the constants in Equation S7 were adjusted in a following study (*222*) of N. America climatologic WTD and soil moisture, using the latitude-longitude-based grid system adopted in digital terrain datasets. Terrain is the main driver of groundwater divergence and convergence, and using the original terrain grid minimizes distortions caused by re-sampling to different projections (such as the one used in RAMS). Consequently a latitude-longitude grid system of 30 arc-sec (~1km) was used (*222*). Because of the finer grid (~1km vs. 1.25km), we had to recalibrate Eq. 7':

$$f = \frac{100}{1+150s}, \quad f>2.5\text{m} \quad \text{(grid=30 arc-sec)} \qquad \text{(S7'')}$$

That is, the apparent steeper slope in the finer grid was compensated by a shallower soil-sediment profile, or a smaller flow cross-section, which reduced groundwater divergence and maintained a higher water table.

Equation S7" does not account for the effect of frozen ground on drainage, and in a subsequent study (*3*) that includes the permafrost regions of Canada and Alaska, we introduced a temperature modifier (Eq. S8) for seasonally frozen and permafrost zones respectively, using simple linear equations of winter air temperature *T*. The parameters in Eq. S8 are calibrated with over ten simulations to compare the simulated wetland area (WTD<0.25 m) with mapped wetlands in northern US and Canada (*3*),

$$fT = 1.5 + 0.1T \qquad (-14\,^oC < T < -5\,^oC,\ fT<=1)$$

$$fT = 0.17 + 0.005T\ (T < -14\,^oC,\ fT>=0.05) \qquad \text{(S8')}$$

These two empirical equations (S7" and S8') are used in the global study here, at the same latitude-longitude projection and grid resolution of 30 arc-second.

First we show the calibration statistics using WTD observations in the temperate N. America, defined by mean January temperature above 5^{o}C. We examine the residual, model water table head (h) minus the observed head (h_o). If there are multiple observations within a 30" model grid cell, the mean is used. The calibration target is a residual distribution that is symmetric with a zero mean and low standard deviation, and low systematic dependence on climate (temperature, precipitation) and terrain (elevation, slope). We present both simulations forced by CLM and Döll-Fiedler recharge.

The residual statistics are shown in Fig. S7 based on 449,728 model cells with observations. On the average, the model water table is 0.04m (CLM) to 1.69m (Döll-Fiedler) lower than observed. The residual histogram (Fig. S7a) is nearly symmetric, but the peak is in the 0-2m bin. We made no attempt to eliminate the shift, because widespread groundwater pumping is known to have lowered the observations (Fig. S1), supported by the fact that the high bias tends to occur at warmer-wetter climate (positive correlation with temperature, Fig. S7b, and precipitation, Fig. S7c), and it also tends to occur on lower and flatter land (negative correlation with elevation, Fig. S7d, and slope, Fig. S7e), because groundwater pumping for irrigation tends to occur in these settings desirable for agriculture.

There is a small negative skew in the residual histogram (longer tail on the left), that is, there are more large negative residuals (simulated water table too low) than positive ones. The correlation plots suggest that the large negative bias tends to occur at cooler and drier climate and higher and steeper terrain. Two clusters of low bias are particularly visible in the plot of residual vs. precipitation (c), with one corresponding to the Rocky Mountains region over the 200-500 mm precipitation range, and the other the Appalachian Mountains region over the 1,000-1,250 mm precipitation range. The reason is that the model grid spacing (30", ~1km) is too coarse to resolve the intricate valleys and to compare with point observations. In nature, the high local relief redistributes the available recharge into the narrow local valleys, creating locally high water table (as observed by the USGS monitoring wells); in the model, the large flat cell only drains to the next flat cell, which, although represents regional drainage well, obliterates local drainage. The above calibration exercise, using observations in temperate N. America, allowed us to obtain the empirical parameters in equations S7" and S8'. We now validate the model over other parts of the world.

S3.2. Evaluation Using Observations from Boreal N. America

The residual statistics based on WTD observations in Boreal N. America (mean January temperature lower than 5^{o}C). The inclusion of the recently obtained large number of observations in Canada allows us to evaluate the model using this independent dataset over a region significantly affected by permafrost and seasonally frozen soils. Figure S8 gives the residual statistics for both simulations.

The most notable difference is the narrower and sharper residual histogram compared to Fig. S7, especially in the simulation forced by Döll-Fiedler recharge. This is due to the tendency of the model to better represent lowland and coastal areas where land drainage is more controlled by groundwater convergence and sea level, and hence less sensitive to recharge and hydraulic parameters (more discussion later). Note that the lack of observations in the deep permafrost further north still leaves the model untested in such settings.

S3.3. Evaluation Using Observations from S. America

Figure S9 gives the residual statistics. Similar to N. America and for the same reasons (pumping and coarse grid resolution in rough terrain), the model water table is higher than observed (positive residual) at low elevations and flat lands, and lower over high and steep terrains. As in N. America, pumping has caused significant water table declines, particularly in eastern Brazil (Fig. S2). Brazilian wells account for ~99% of the observations, and of which ~95% are pumping wells themselves.

S3.4. Evaluation Using Observations from Europe and Africa

Figure S10 gives the residual statistics for the two simulations. The dense spatial coverage and the long records (most over several decades) in Western Europe reduced the spatial gaps and temporal noises in the observations, contributing to the narrow and tall histograms (note the 4 times higher vertical axis than Fig. S9). The high bias tends to occur in flat terrains (e), again attributable to pumping; widespread pumping for water supply and improving land drainage is documented in the Netherlands (*36*) and in Germany where 70% of drinking water is obtained from the shallow aquifers (http://www.bgr.bund.de/EN/Themen/Wasser/wasser_node_en.html).

As shown in Fig. S6 which compares model and observations at the individual observation sites in Europe, the model is closer to observations where the water table is shallow (the Netherlands, Germany, and along coastlines), where the water balance is strongly controlled by groundwater convergence from the neighbors (plentiful source) and topography and sea level (water table cannot be above land surface or below the sea level, putting predictable constraints). But over groundwater divergent regions where the water table is deep, the water balance is more sensitive to pumping, recharge and hydraulic parameters. The presence of shallow water table in the Netherlands and northern Germany, in addition to the dense and long-term observations, also contributed to the narrower residual histograms in Fig. S10.

S3.5. Evaluation with Observations from Australia and Asia

Figure S11 gives the residual statistics. Unlike the other continents, the simulated water table on the average is substantially lower than observed (CLM 5.08 m lower, and Döll-Fiedler 8.92 m lower). The low bias largely occurs in temperate climates and over moderate slopes. One likely reason is that the observations are made in shallow artisan aquifers where the groundwater is under higher pressure than phreatic conditions (e.g., some of the wells report water levels up to 38m above land surface), and another reason is the widely reported perched water table in the wet season (some due to irrigation) which is elevated above the mean regional water table. These data points are difficult to remove because most of the state-territory databases in Australia do not differentiate the aquifer types and/or report well depths. It is also likely that both water table recharge estimates are biased low over Australia. At the present, we need to keep in mind in the subsequent analyses that the simulated water table depth can be on the lower side over this continent.

Table 1 summarizes the residual statistics of the five continental regions forced by both recharge estimates, as well as the global statistics (graphs similar to Fig. S7-S11 and hence not shown). For the global statistics, only the results from Döll-Fiedler recharge is shown, but

differentiations are made between regions of observed shallow (<5 m) and deep water table (>5 m), for the purpose of evaluating the model in different groundwater regimes (convergent vs. divergent). Over all continents, the CLM recharge gives a higher (or shallower) water table than Döll-Fiedler recharge. Globally, the model forced by Döll-Fiedler recharge is on the average 1.62 m deeper than observed, and it tends to perform better in shallow water table regions (higher and narrower histogram, or lower standard deviation). Since our estimates of groundwater-affected ecosystems focus on the shallow end of the water table distribution, it is encouraging that the model performs better here.

Given the minimal model construct (Darcy's law and mass balance), simple permeability function (exponential decay in depth depending on terrain slope and winter temperature), the lack of real and local permeability data that affects the local water table height, the scale difference between model and observations (1 km grid cell vs. a well point), the large temporal noise in the observation (each data point has a different time stamp), and the effect of groundwater pumping and drainage on the observations, we consider the global simulations here adequate for the purpose of understanding large-scale features in water table depth and the influence of climate, terrain and sea-level drivers.

S4. Detailed Maps of Simulated WTD and Ramsar Wetlands

Below we present the continental maps of simulated WTD showing more details than the global map of Fig. 3. Smaller zoomed-in images give examples of WTD relationship to land ecosystems. On the maps we also marked the 85 largest (>5,000 km^2) of the 2,048 Ramsar Wetlands of International Importance (http://www.ramsar.org/cda/en/ramsar-documents-list/main/ramsar/1-31-218_4000_0__) recognized for their "significance in terms of ecology, botany, zoology, limnology and hydrology". They are listed in Table S2, ranked by protected area within each continent. Note that the area shown are the protected (not the full) area extent, which is the reason that the largest ones are found in undeveloped regions such as Africa where natural wetlands are largely intact; in the industrialized world, natural wetlands have been encroached by human activities; for example, ~53% of the natural wetlands in the lower 48 states of the US have been destroyed since European settlement (*223*). These Ramsar wetlands are shown here to illustrate the link between shallow water table and land drainage. Large and ecologically valuable wetlands are found in the arid Sahara and Sahel of Africa, for example, not attributed to climate but to land drainage.

S5. Water Table Depth as a Wetland Indicator

In an earlier study (*3*) we provided a literature review and synthesis of hydrologic mechanisms of wetland formation regarding the role of shallow groundwater; the latter supports surface-water-fed wetlands by maintaining a saturated substrate (inhibiting infiltration loss) or directly feed wetlands in regional discharge zones. This is the reason that the water table map closely resembles the wetland map at continental to hillslope-valley scales (*3*, and Figs. S12-S16). Here we delineate wetlands from the simulation as grid cells where the water table is within 0.25m of land surface based on the literature survey (*3*) over N. America where wetlands are mapped in details. Figure S17 plots such obtained wetland area with mapped wetlands in Alaska and Canada (top) and the lower 48 states of the US (bottom, pre-development or natural wetlands, *223*), from the simulation using CLM recharge (left) and Döll-Fiedler recharge (right), with Pearson correlation-coefficient shown. Canada and Alaska wetlands are plotted separately because they are affected by frozen grounds.

S6. Estimating Global Land Areas Potentially Affected by Shallow Groundwater

Although CLM gives a better residual statistics, Döll-Fielder gives a closer estimate of wetland extent. Döll-Fielder also has a lower recharge bias in arid regions, and hence will be used for the estimates here. The WTD distributions are shown for both in Table S3.

Based on the Döll-Fielder run, 14.5% of the simulation domain has a mean water table at the land surface (WTD=0). These are model grid cells receiving persistent groundwater discharge (springs) that raise the water table above land surface, but reset at the land surface in the simulation at each iteration step (to simulate evaporation and river removal). They best represent groundwater-fed aquatic ecosystems including rivers, lakes (excluding the large ones whited out in Figs. S12-S16) and perennially inundated wetlands. However, it is difficult to separate out the area covered by wetlands from this category because individual grid cells (~1 km wide) may contain channels and lakes (deeper surface water) and riparian wetlands (shallow water, with emergent vegetation). Although finer model grids can more explicitly resolve the finer features, the conceptual difficulty of drawing a line between aquatic and wetland ecosystems remains, in both models and the real world, because definitions vary and the water levels in the rivers/lakes rise and fall and their areas expand and contract. So we interpret this 14.5% area as mostly aquatic environments.

The next WTD bin in Table S3 (0-0.25 m) best represents wetlands that are less frequently inundated but characterized by a persistent shallow water table and anoxic soil conditions that select a special class of vegetation. About 1.8% of global land area falls into this category. This, plus the unknown portion of the inundated wetlands in the first category, would add up to the total global wetlands, the estimate of which ranges from 4% to 12% as reported in the literature (*224*).

The next three WTD bins (0.25-3 m) roughly correspond to the rooting depths of upland vegetation (*225*). At this depth range, the water table can either supply plant roots directly or by upward capillary flux from the water table indirectly. However, patterns in plant rooting depths are complex and a single cut-off value is difficult to justify; although most plants have 50% of the root mass within the top 30 cm and 95% within the top 2 m soil (*225*), the maximum rooting depth can reach tens of meters in arid climates (*226*). Given this, we consider three possible rooting depths (1, 2, and 3 m) in estimating global land area where groundwater is within the rooting depths. The three rooting depths give 5.3%, 10.9% and 15.9%, respectively, of the global land area.

Taken together, the aquatic, wetland and upland ecosystems that are potentially supported by shallow groundwater would amount to 22%, 27%, and 32% of the global land area corresponding to the threshold water table depths of 1, 2, and 3m. These three estimates also reveal the sensitivity of groundwater-affected area to the choice of the threshold.

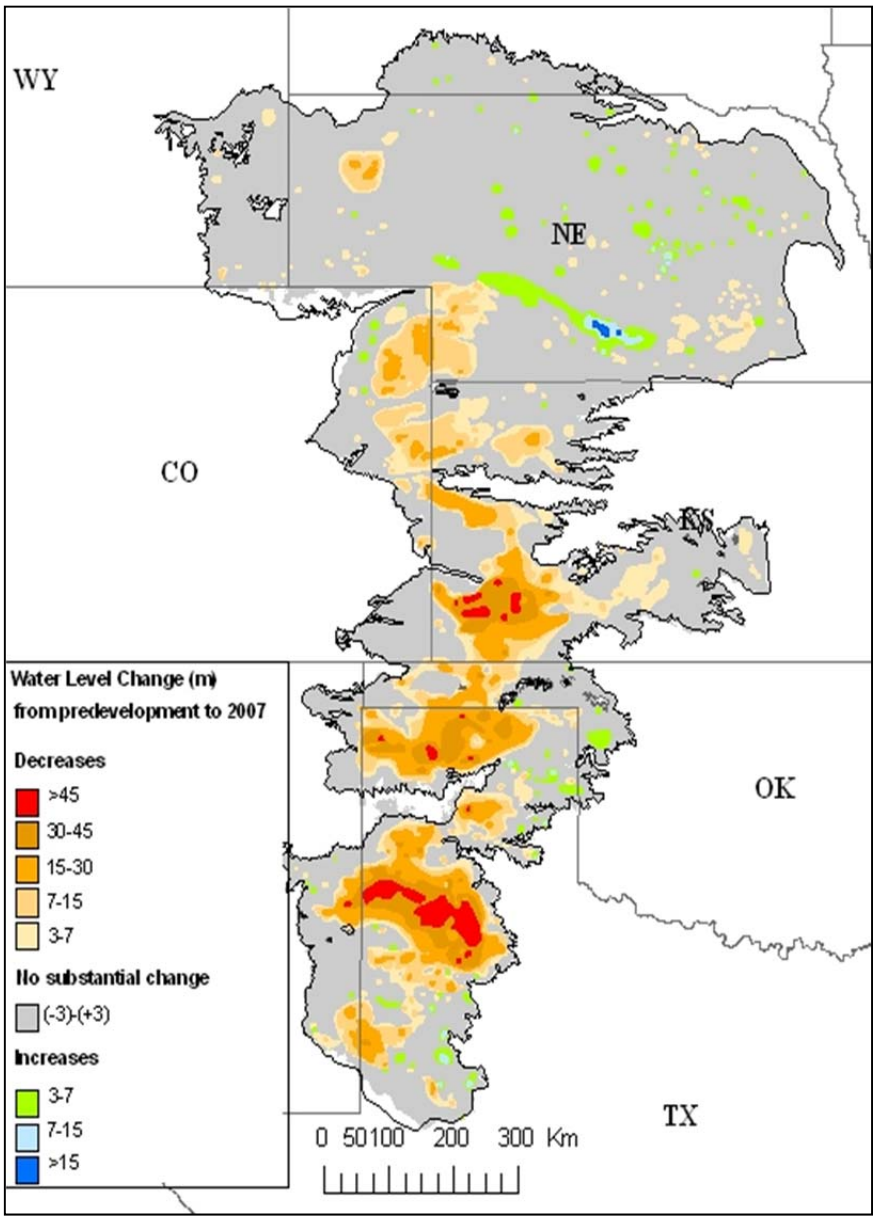

Fig. S1. Water table decline in the US High Plains from groundwater pumping (*35*).

Fig. S2. Principle aquifers in Brazil (names in grey lettering) with groundwater depletion indicated by the ratio of withdraw over renewal (red numbers), and Amazonian cities (names in orange lettering) partially or entirely supplied by groundwater (http://www.ana.gov.br/pnrh_novo/documentos/01%20Disponibilidade%20e%20Demandas/VF%20DisponibilidadeDemanda.pdf).

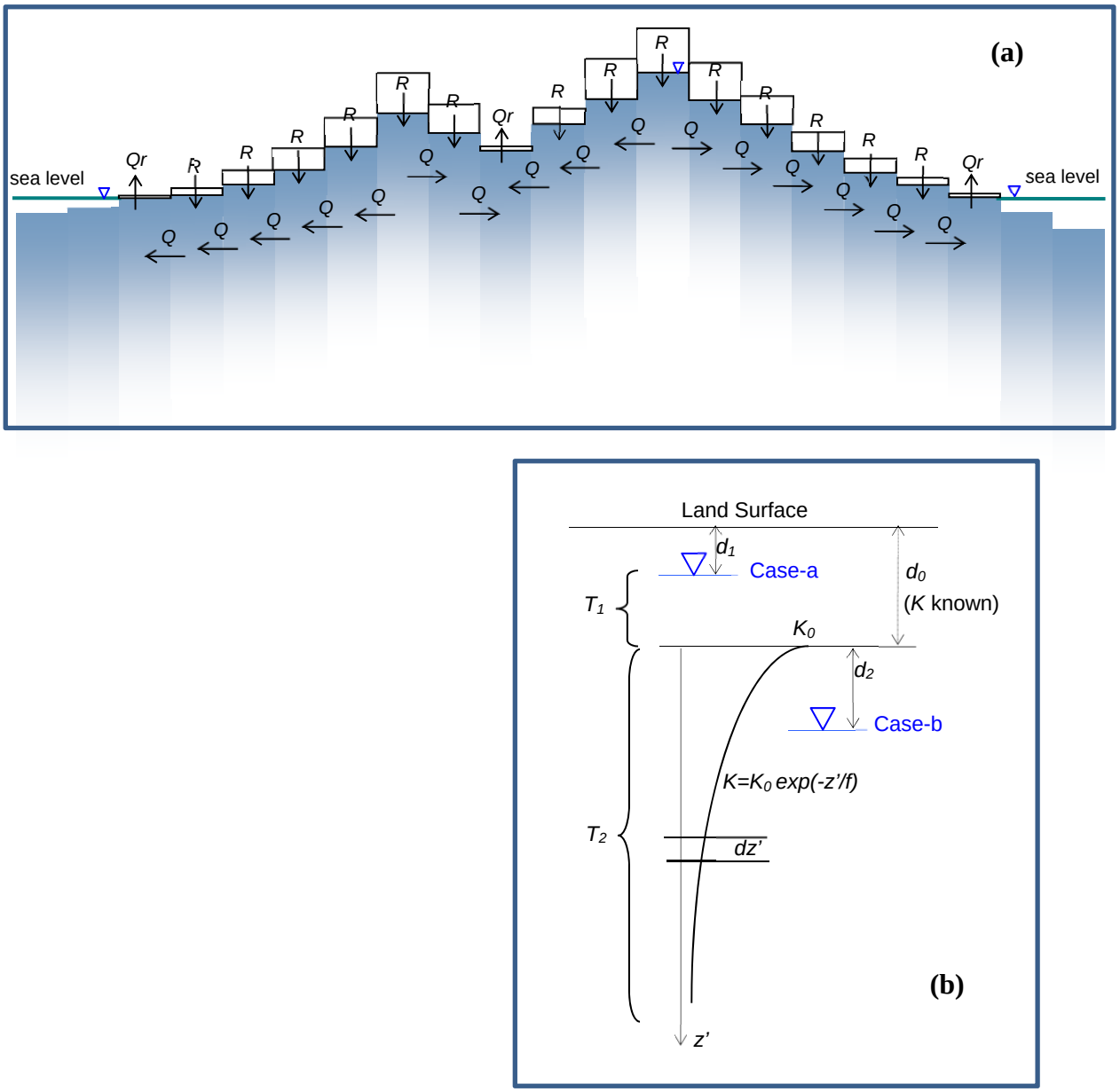

Fig. S3. (a) Schematic groundwater flow model to simulate the interplays of climate (recharge *R*), terrain (lateral convergence *Q*) and sea level (boundary condition) on water table depth over a continent. Over a hill-top grid cell, R feeds divergence; in a valley or coastal grid cell, convergence feeds rivers, lakes, and wetlands, (b) Details in calculating groundwater flow transmissivity, *T*, for Case-a, water table within the depth of known soil hydraulic conductivity (*K*), and Case-b, water table below the known depth from which *K* is assumed to decrease exponentially with depth.

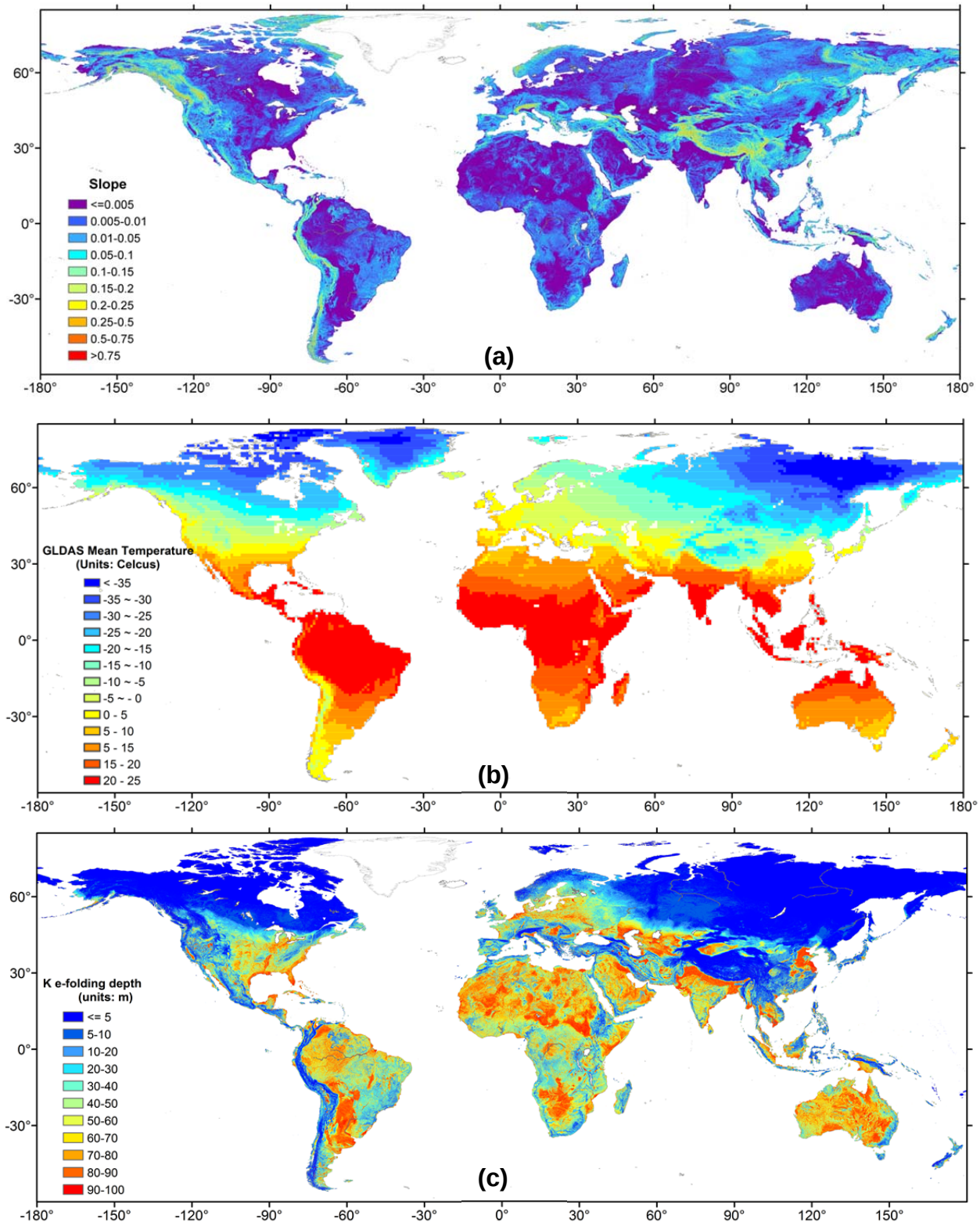

Fig. S4. (a) Terrain slope at 30 arc-second grids, (b) 30yr mean January air temperature, (c) the e-folding depth of exponential decrease in K with depth.

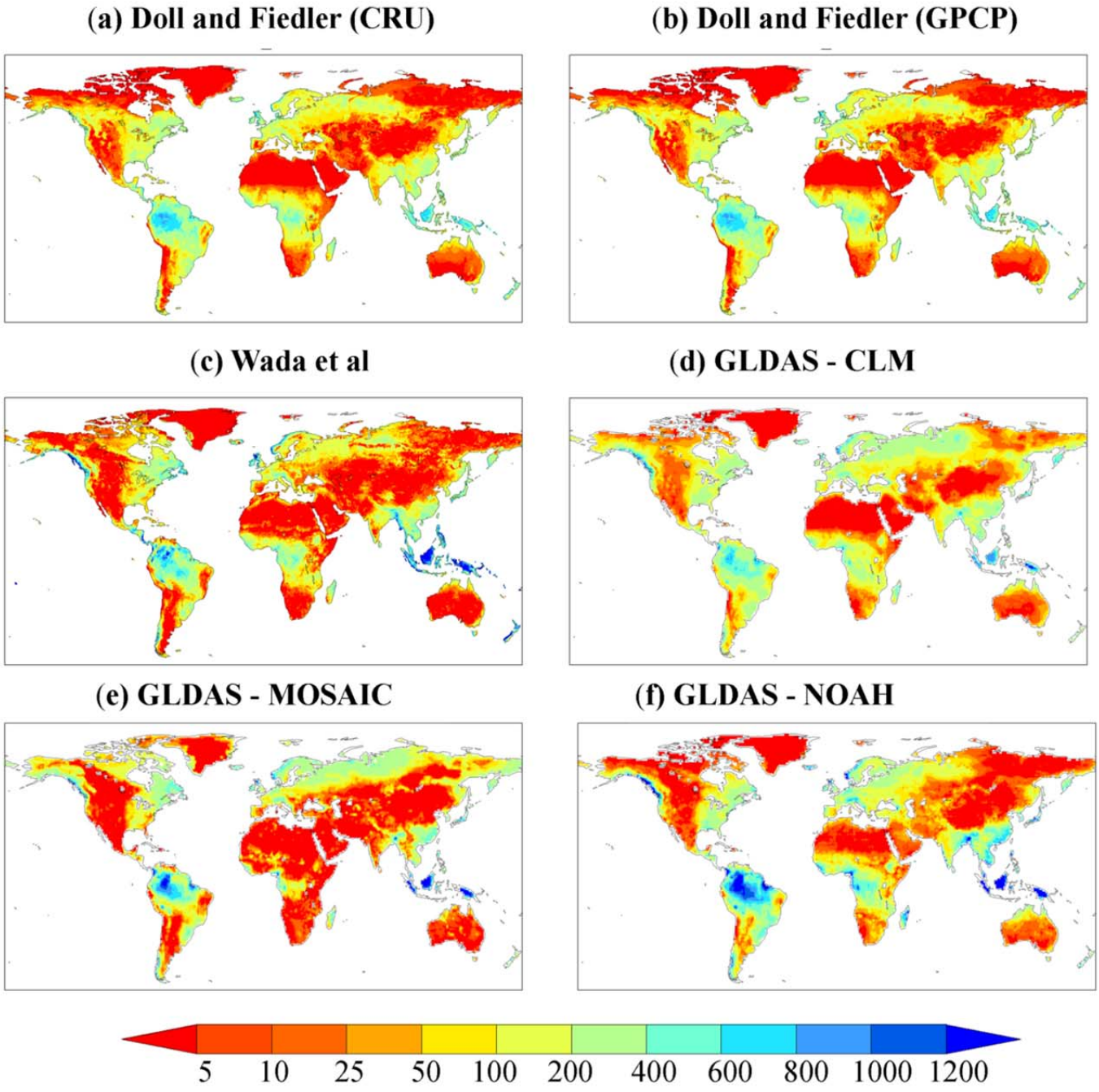

Fig. S5. Global mean annual recharge estimates in mm/yr: (a) by Döll-Fiedler forced by CRU global precipitation dataset, (b) by the same authors but forced with GPCP precipitation dataset, (c) by Wada-et-al, (d) by GLDAS-CLM model, (e) by GLDAS-MOSIAC model, and (f) by GLDAS-NOAH model.

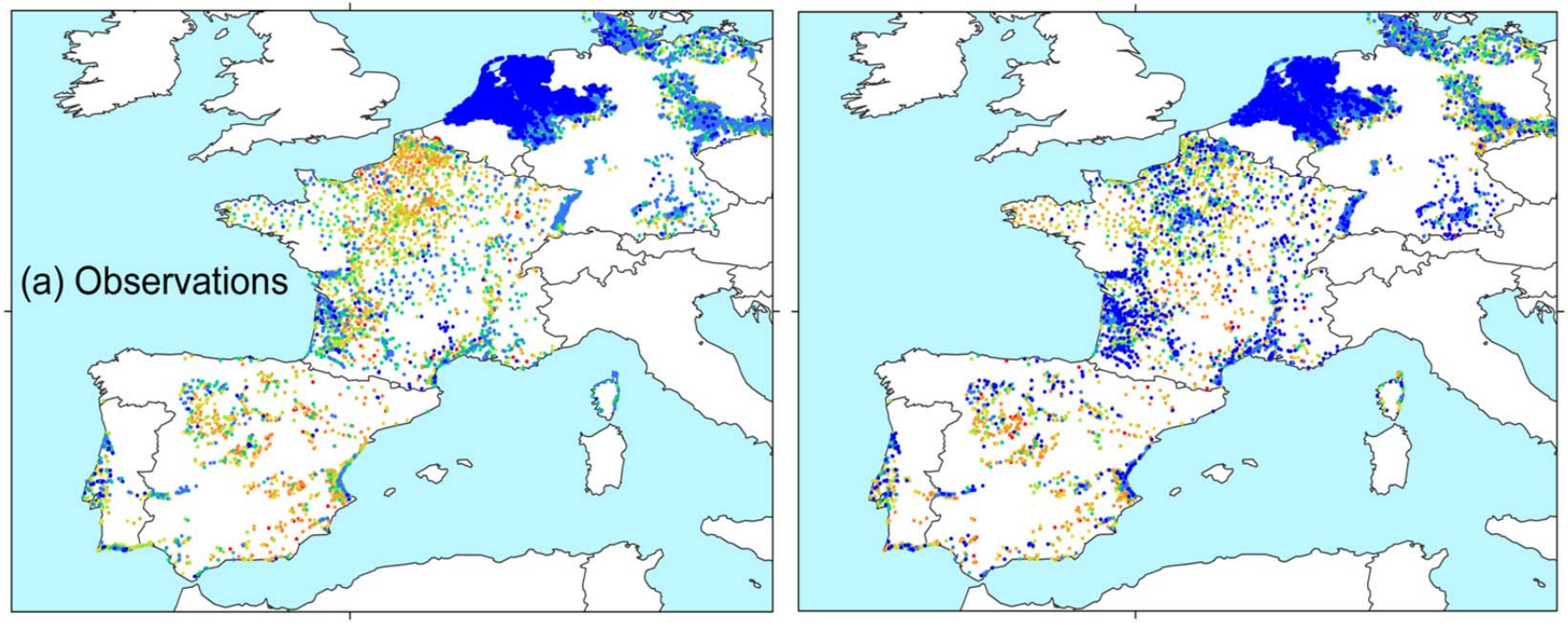

Fig. S6. Visual comparison of observed (a) and modeled (b) WTD at model grid cells with observations over Western Europe. The model simulation is forced by Döll-Fiedler recharge.

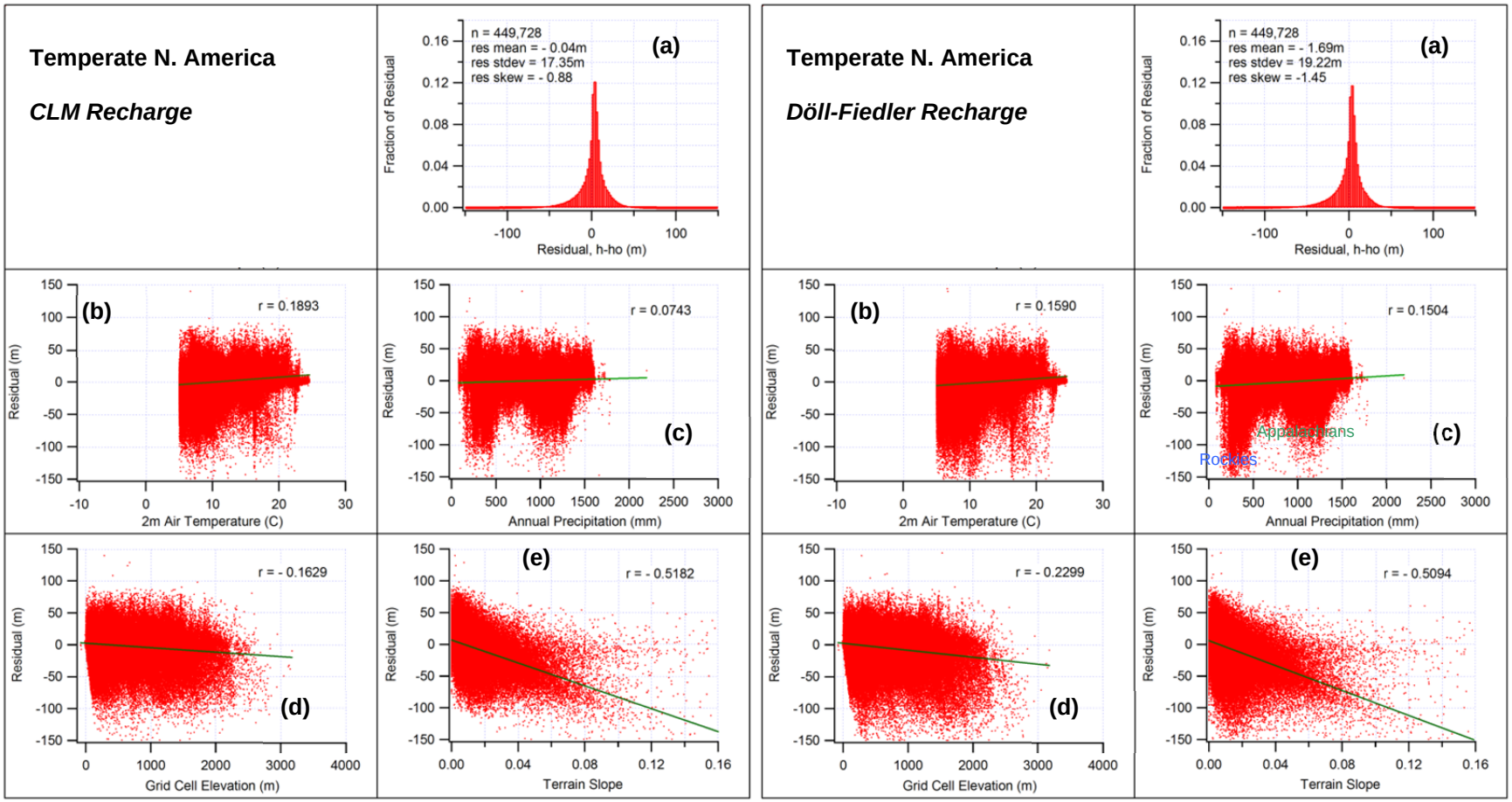

Fig. S7. Residual statistics for the calibration forced by CLM recharge (left) and Döll-Fiedler recharge (right) over temperate N. America: (a) histogram of the residual with mean, standard deviation and skew, (b) residual vs. annual mean air temperature, (c) residual vs. annual mean precipitation, (d) residual vs. grid cell elevation, and (e) residual vs. terrain slope. Pearson correlation coefficient, r, is shown for (b) to (e).

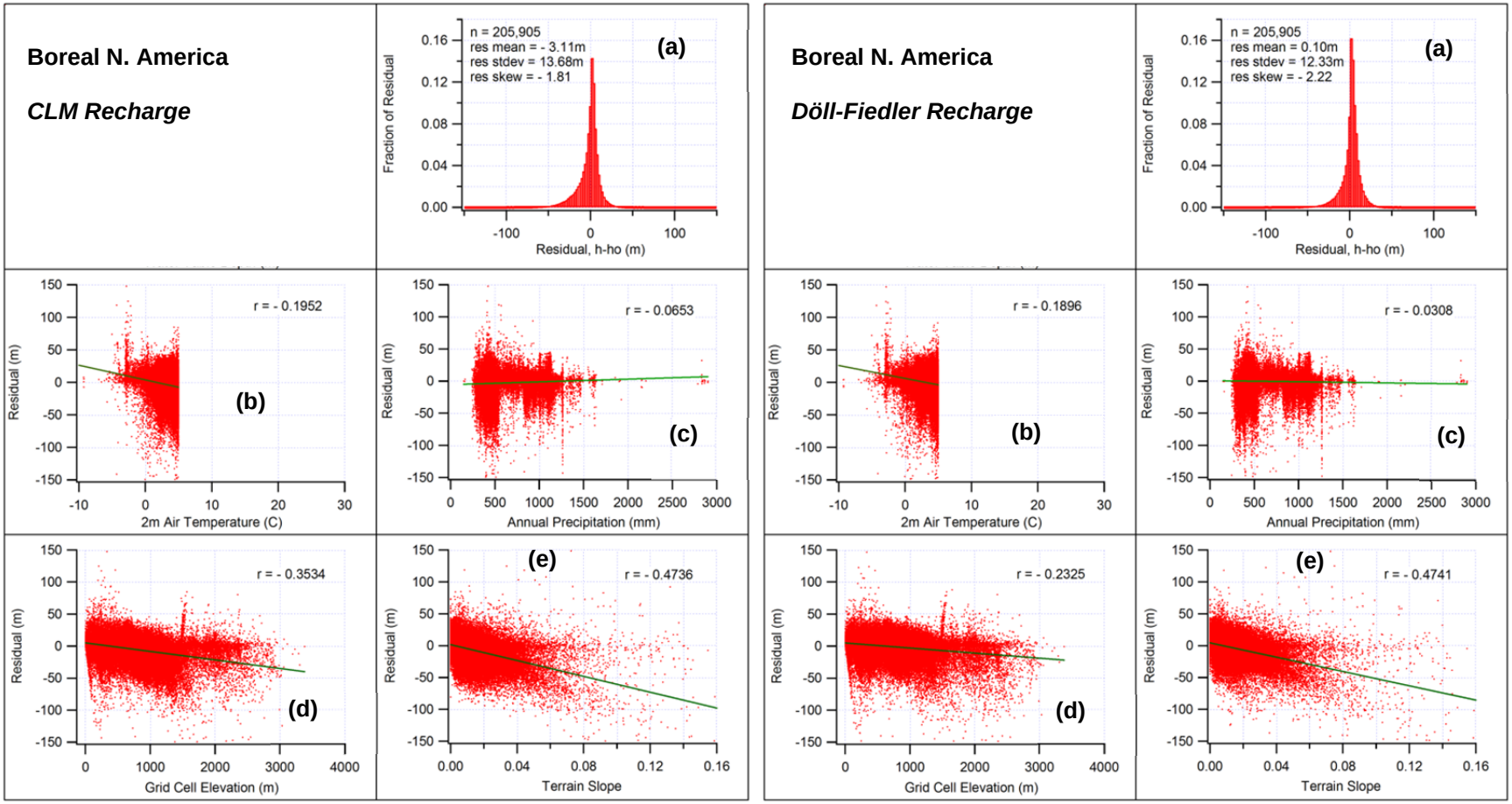

Fig. S8. Residual statistics for the calibration forced by CLM recharge (left) and Döll-Fiedler recharge (right) over boreal N. America: (a) histogram of the residual with mean, standard deviation and skew, (b) residual vs. annual mean air temperature, (c) residual vs. annual mean precipitation, (d) residual vs. grid cell elevation, and (e) residual vs. terrain slope. Pearson correlation coefficient, r, is shown for (b) to (e).

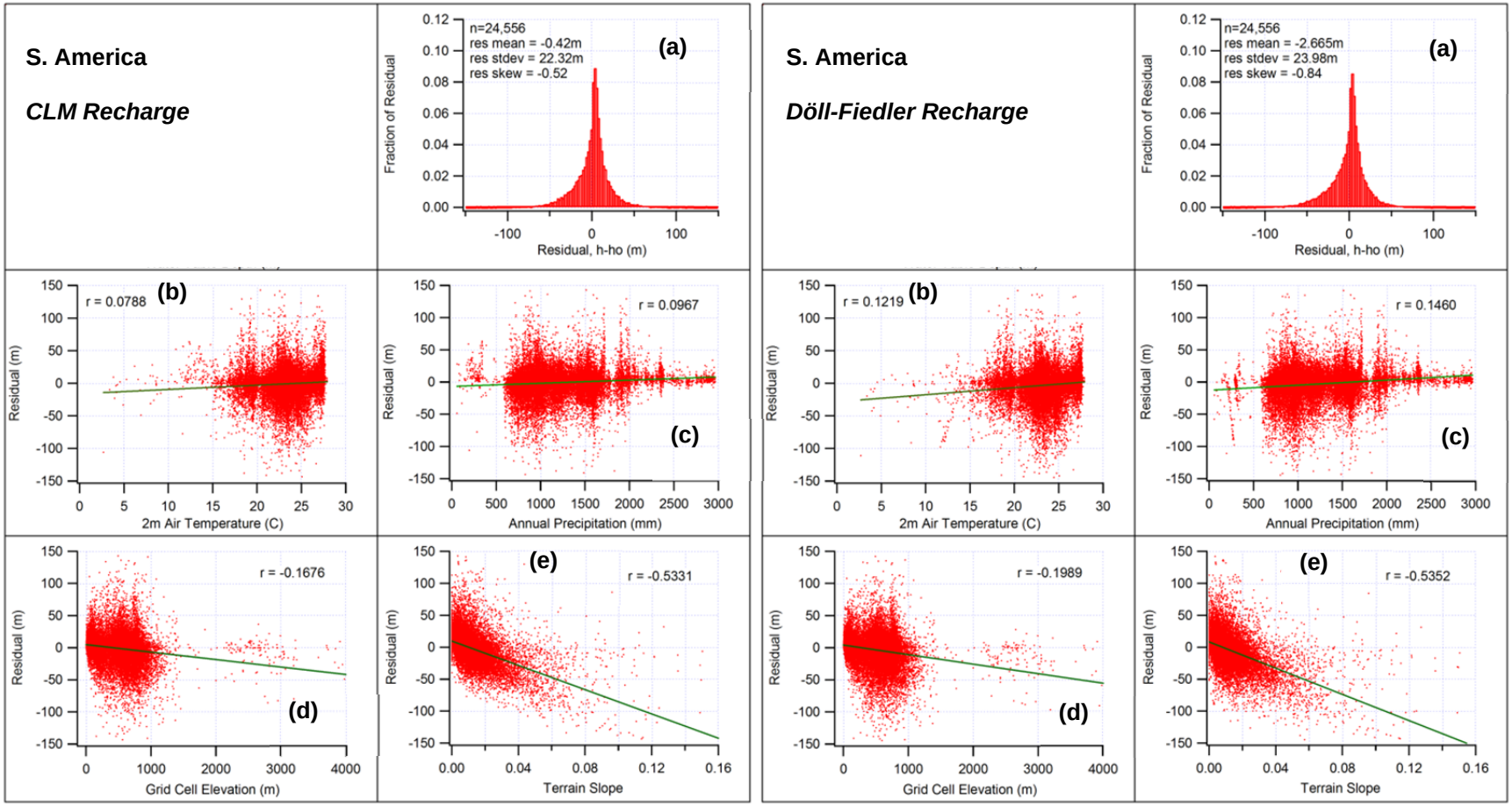

Fig. S9. Residual statistics for the calibration forced by CLM recharge (left) and Döll-Fiedler recharge (right) over S. America: (a) histogram of the residual with mean, standard deviation and skew, (b) residual vs. annual mean air temperature, (c) residual vs. annual mean precipitation, (d) residual vs. grid cell elevation, and (e) residual vs. terrain slope. Pearson correlation coefficient, r, is shown for (b) to (e).

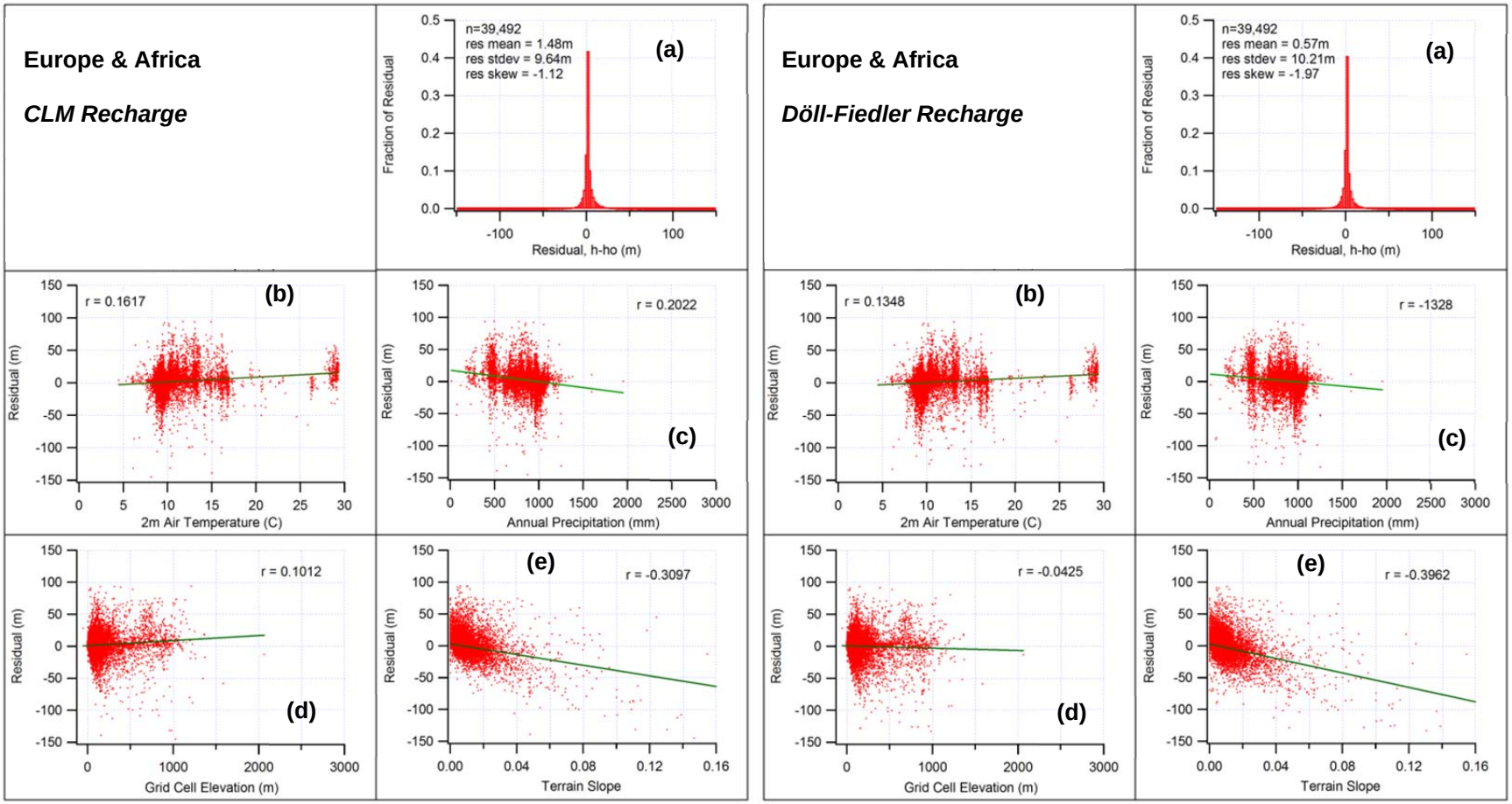

Fig. S10. Residual statistics for the calibration forced by CLM recharge (left) and Döll-Fiedler recharge (right) over Europe and Africa: (a) histogram of the residual with mean, standard deviation and skew, (b) residual vs. annual mean air temperature, (c) residual vs. annual mean precipitation, (d) residual vs. grid cell elevation, and (e) residual vs. terrain slope. Pearson correlation coefficient, r, is shown for (b) to (e).

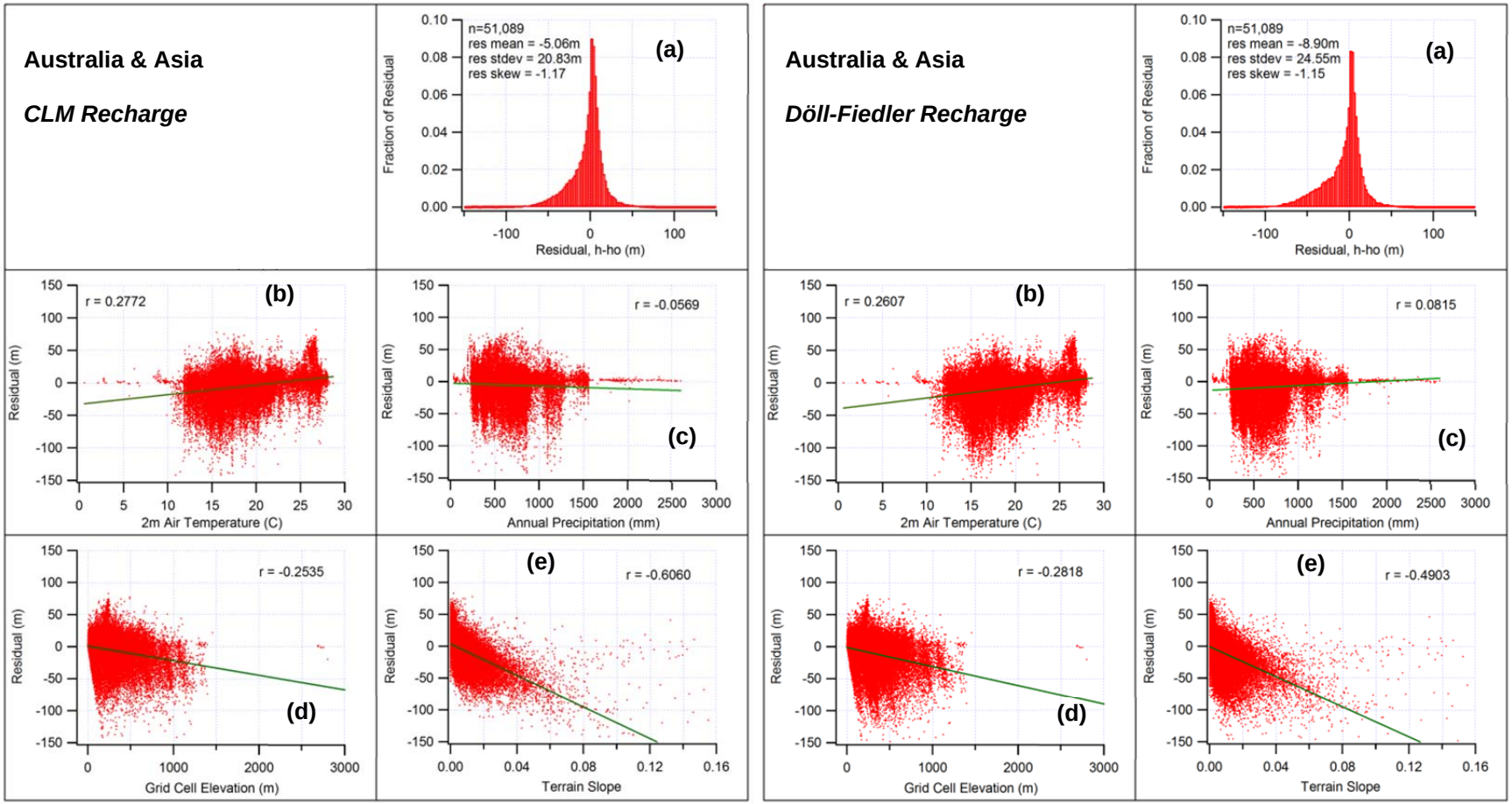

Fig. S11. Residual statistics for the calibration forced by CLM recharge (left) and Döll-Fiedler recharge (right) over Australia and Asia: (a) histogram of the residual with mean, standard deviation and skew, (b) residual vs. annual mean air temperature, (c) residual vs. annual mean precipitation, (d) residual vs. grid cell elevation, and (e) residual vs. terrain slope. Pearson correlation coefficient, r, is shown for (b) to (e).

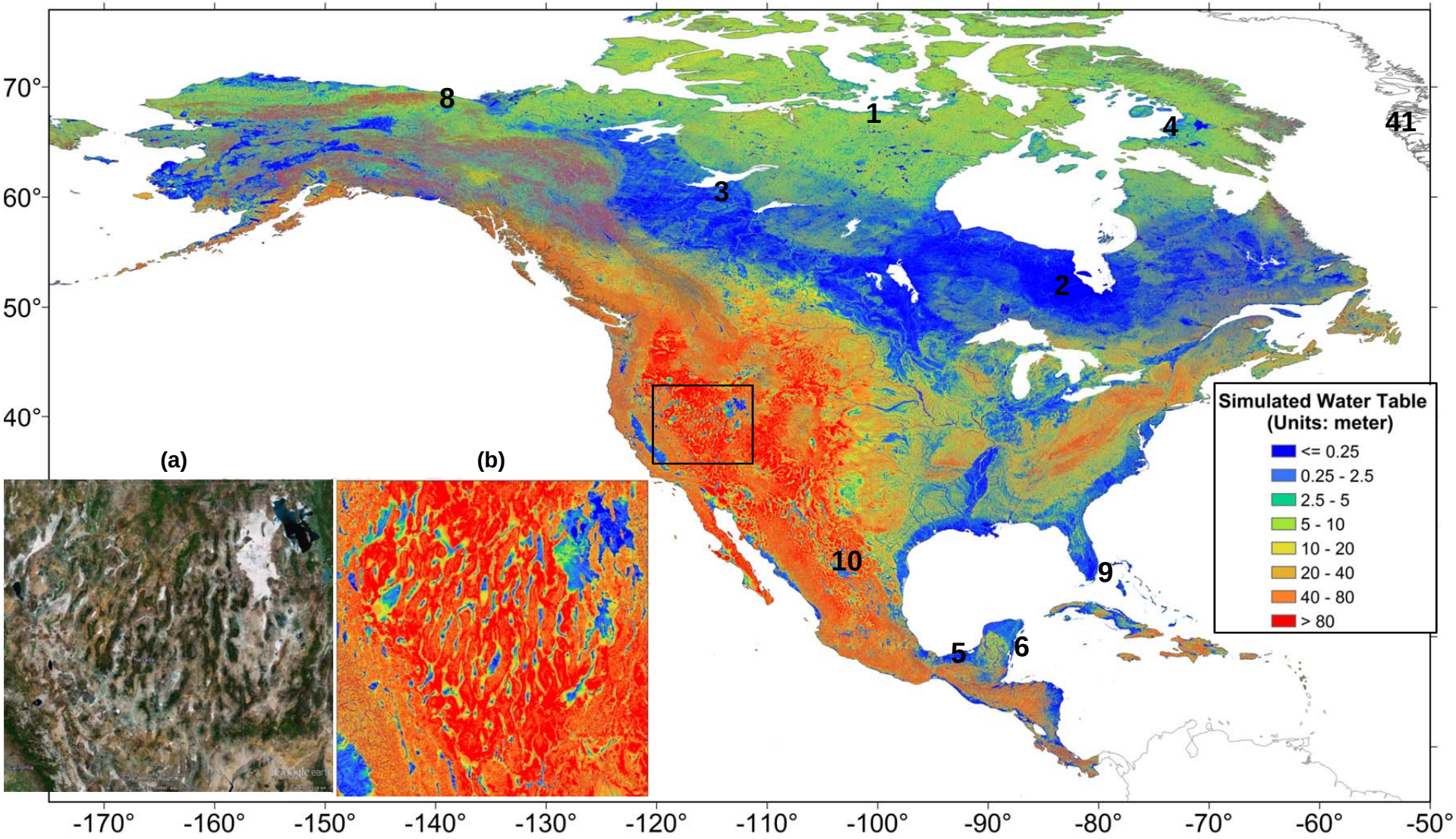

Fig. S12. Simulated WTD in N. America. (a) Salt lakes/playas in the intermountain valleys (some with white salt crust observable from space). (b) Corresponding model WTD. The numbers mark the largest (top 85) Ramsar wetlands on this continent (Table S2). The stripes north of 60^{o}N are from ASTER digital topography data.

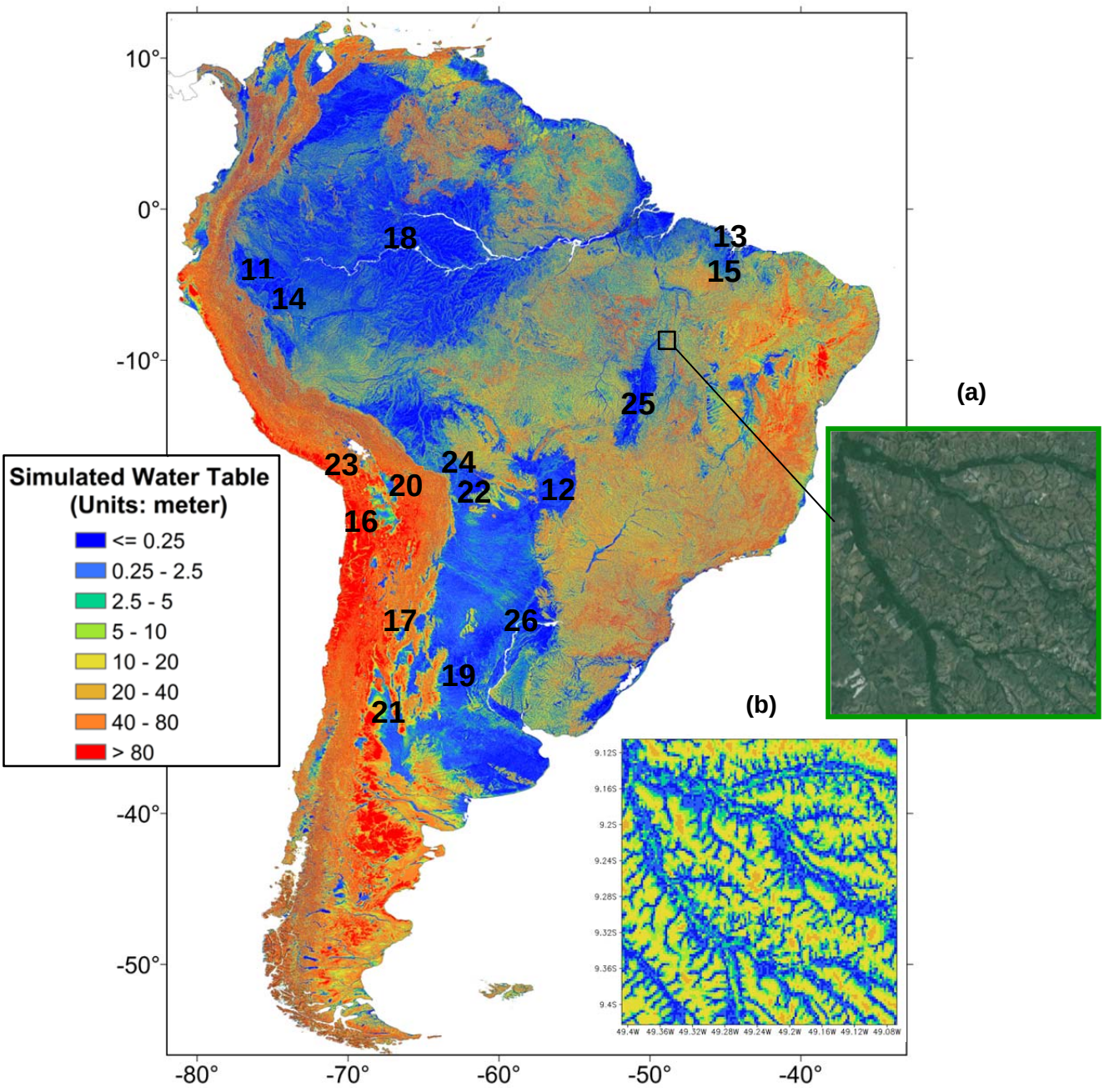

Fig. S13. Simulated WTD in S. America, showing (a) the gallery forests along valleys carved into the Brazilian shields, (b) modeled WTD over the same region showing groundwater seeps at the base of the slopes. The numbers correspond to the top 85 largest Ramsar wetlands found on this continent (Table S2).

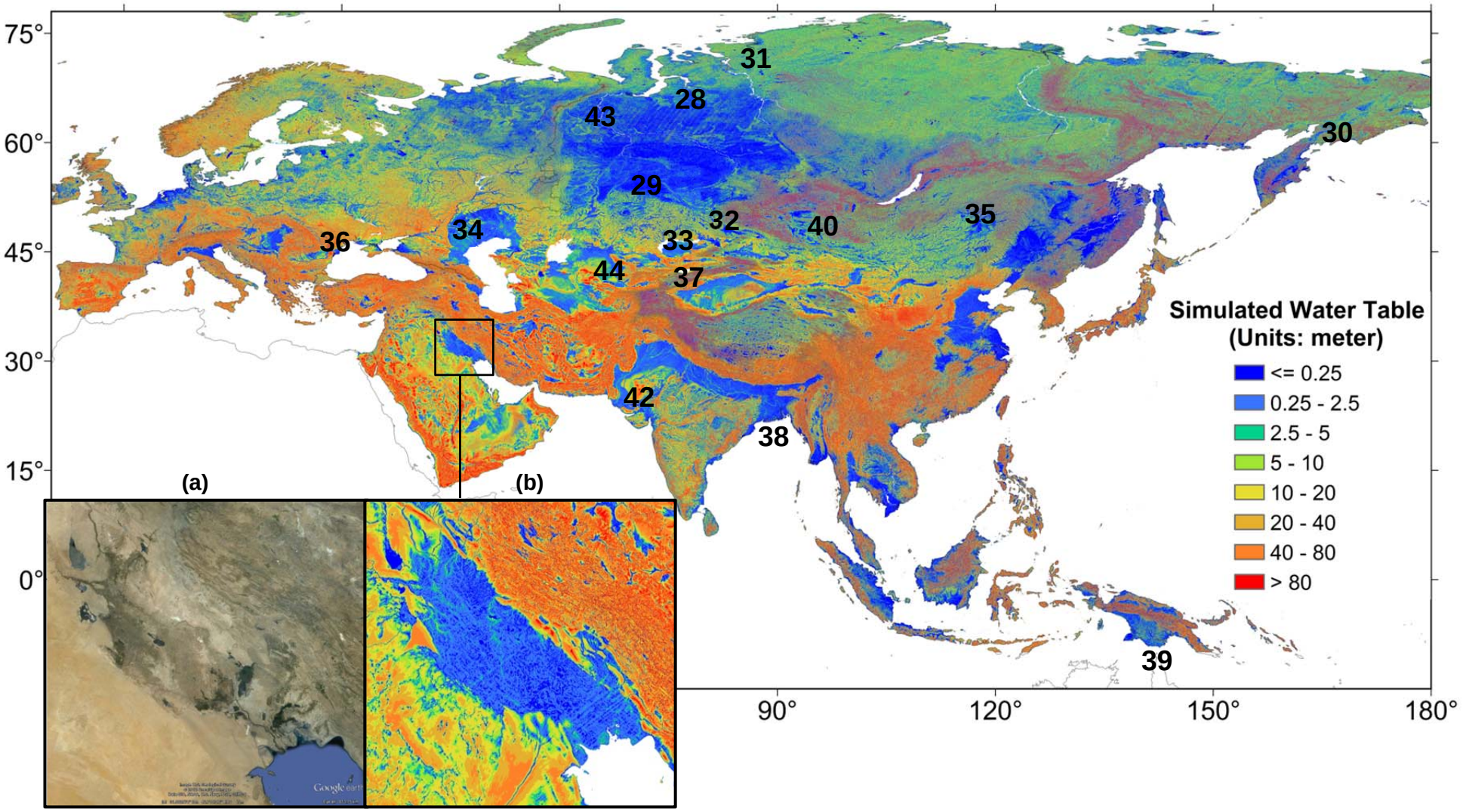

Fig. S14. Simulated WTD in Europe and Asia showing the Mesopotamian Marshes of Iraq and Iran on the Persian Gulf coast (a) and the corresponding WTD (b). The numbers indicate the world's 85 largest Ramsar wetlands found on this continent (Table S2). The stripes north of 60°N are from ASTER digital topography data.

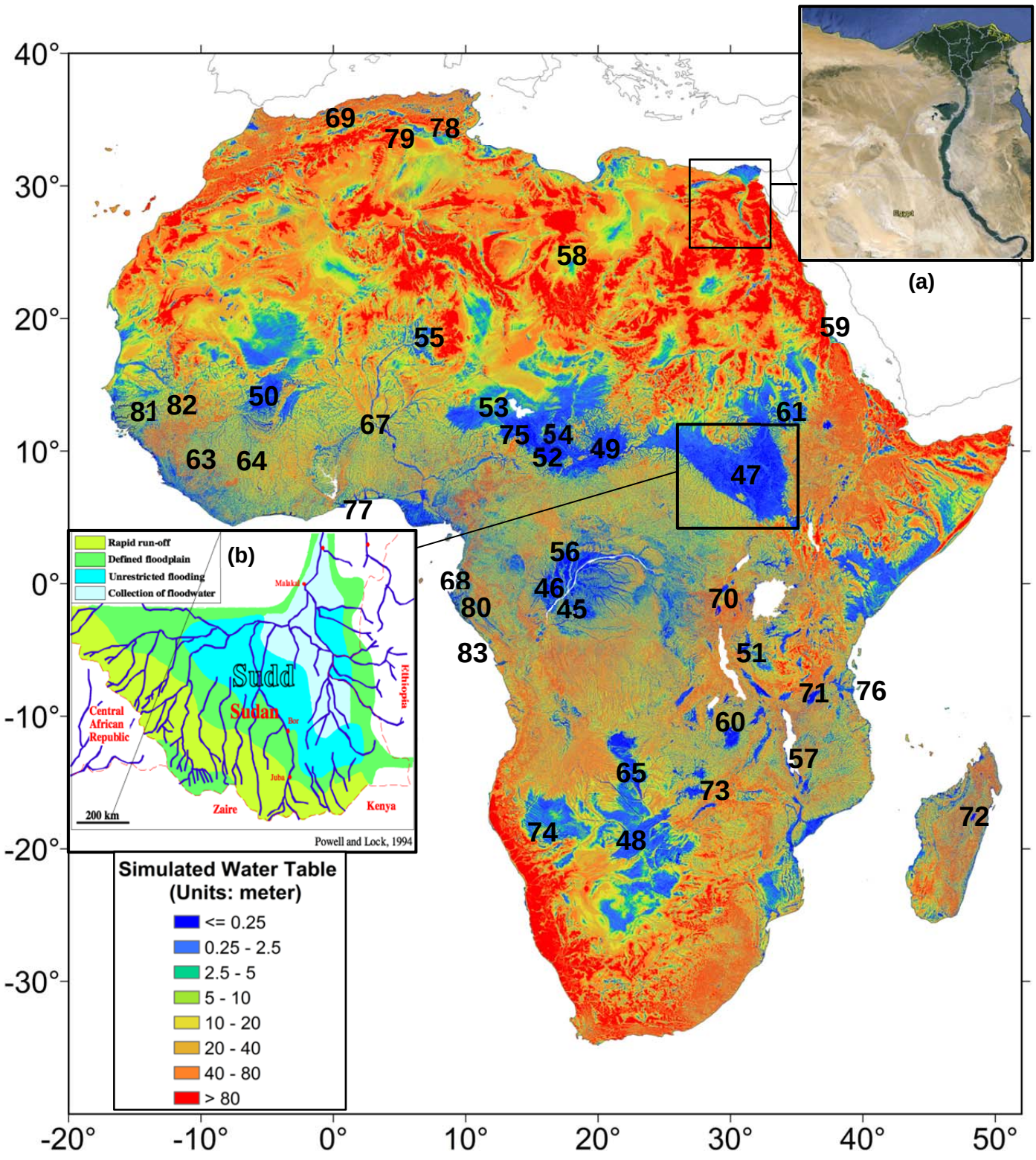

Figure S15. Simulated WTD in Africa, showing the oases in the lower Nile (a) and the flooding characterisics of the Sudd Swamps (b) (*227*), also described as the Great Marsh of the White Nile (*228*). The numbers indicate the world's 85 largest Ramsar wetlands found on this continent (Table S2).

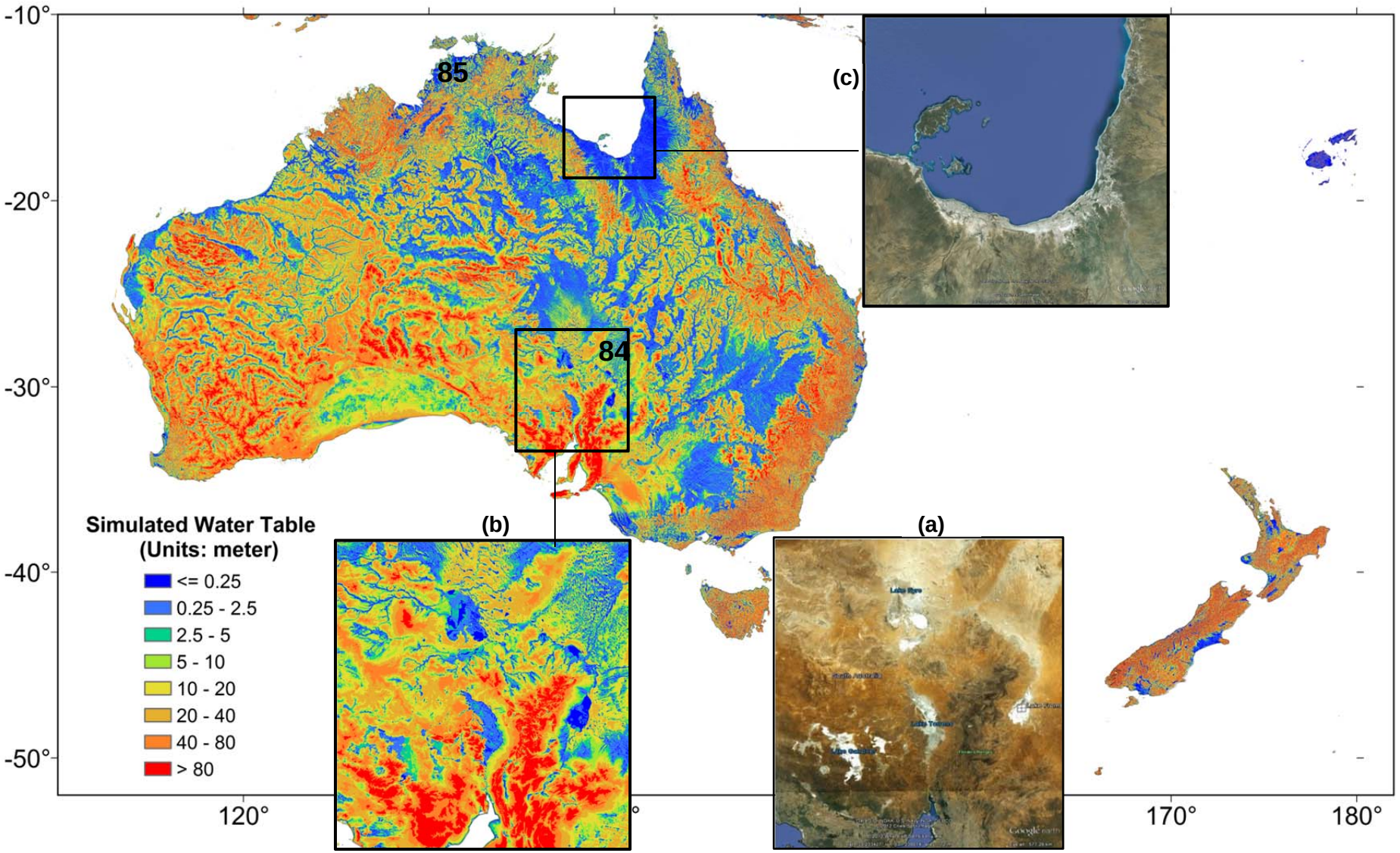

Figure S16. Simulated WTD in Australia and New Zealand, showing the four largest salt lakes in South Australia (a) and the corresponding WTD (b) where evaporation from the shallow water table accumulates salt forming white crusts observable from space. Salt crust also forms along the Gulf of Carpentaria (c) where the WT is near the land surface. The numbers mark the world's 85 largest Ramsar wetlands found on this continent (Table S2).

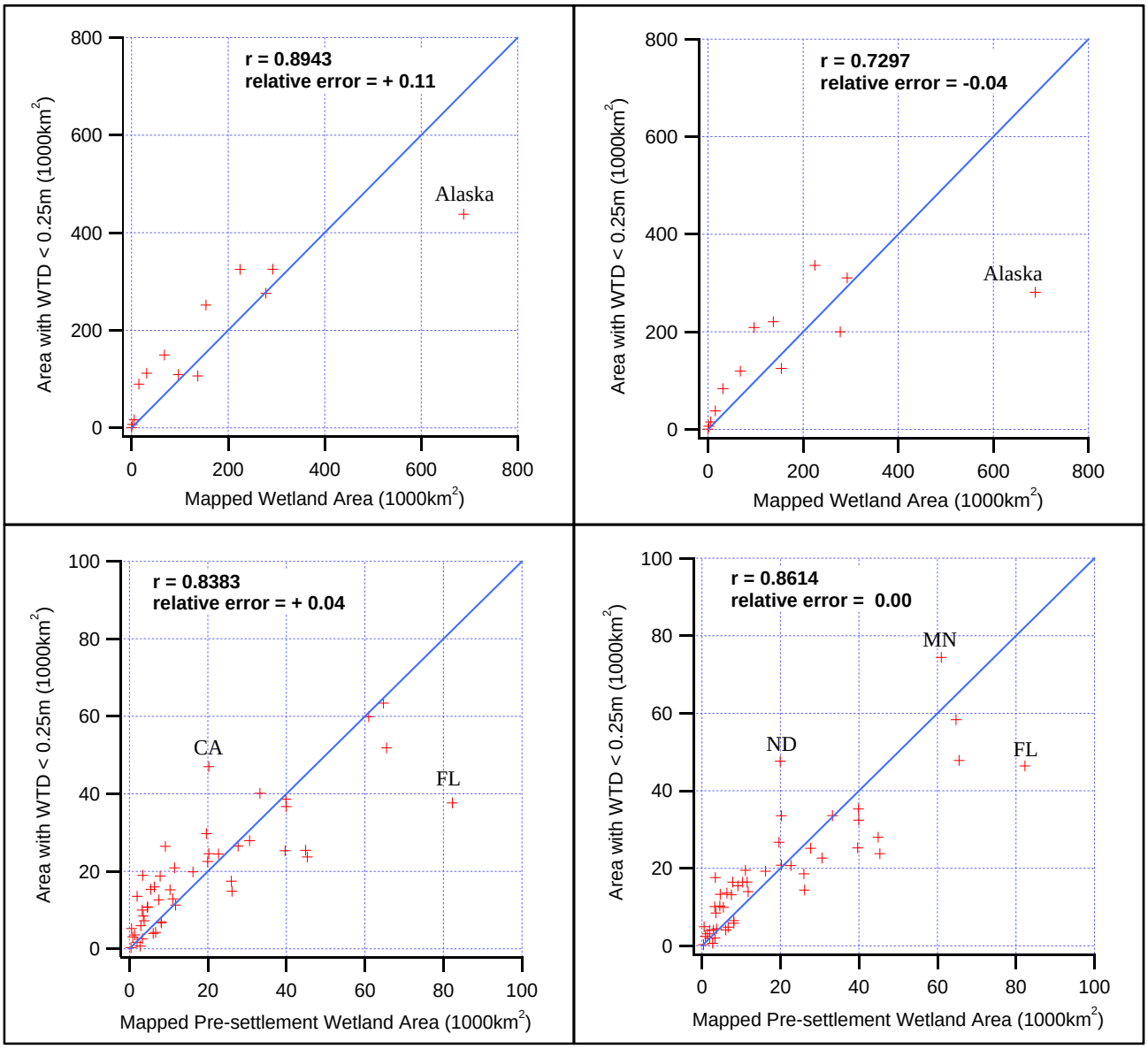

Figure S17. WTD defined wetlands vs. mapped natural (pre-settlement) wetlands for the lower 48 states of US (bottom), and Alaska and Canada (top), forced by CLM3 recharge (left) and Döll-Fiedler recharge (right).

Table S1. Summary of residual statistics over four continental regions forced by two recharge estimates.

Residual Stats	North America				South America		Western Europe & Africa		Australia & Asia		Global		
	Temperate Region		Cold Region								Total	Shallow WTD	Deep WTD
	CLM	Döll-Fiedler	CLM	Döll-Fiedler	CLM	Döll-Fiedler	CLM	Döll-Fiedler	CLM	Döll-Fiedler	Doll-Fiedler Recharge		
# cells with obs.	449,728	449,728	205,905	205,905	24,556	24,556	39,492	39,492	51,126	51,126	770,303	314,152	456151
Mean (m)	-0.04	-1.69	-3.11	0.10	-0.42	-2.67	1.48	0.57	-5.08	-8.92	-1.62	-5.47	1.03
St. dev. (m)	17.35	19.22	13.68	12.33	22.32	23.98	9.64	10.21	20.85	24.56	17.91	14.22	19.62
Skew	-0.88	-1.45	-1.81	-2.22	-0.52	-0.84	-1.12	-1.97	-1.17	-1.15	-1.86	-3.41	-1.68
Corr. to temp	0.1893	0.1590	-0.1952	-0.1896	0.0788	0.1219	0.1617	0.1348	0.2779	0.2612	0.0098	-0.1114	0.0303
Corr. to precip.	0.0743	0.1504	-0.0653	-0.0308	0.0967	0.1460	0.2022	-0.1328	-0.0570	0.0812	0.0940	0.0597	0.1150
Corr. to elevation	-0.1629	-0.2299	-0.3534	-0.2325	-0.1676	-0.1989	0.1012	-0.0425	-0.2530	-0.2816	-0.1902	-0.2469	-0.2042
Corr. to slope	-0.5182	-0.5094	-0.4736	-0.4741	-0.5331	-0.5352	-0.3097	-0.3962	-0.6058	-0.4904	-0.4869	-0.6154	-0.4799

Table S2. World's 85 largest (>5,000 km^2) Ramsar Wetlands of International Importance. Within each continent, they are ranked by the protected area extent. Where a wetland spans more than one country, the contributions are shaded and the total area obtained.

	Wetland	Country	State	Protected Area (km2)	Latitude	Longitude
North America						
1	*Queen Maud Gulf*	Canada	Northwest Territories	62,782	67.00	-102.00
2	*Polar Bear Provincial Park*	Canada	Ontario	24,087	52.50	-84.50
3	*Whooping Crane Summer Range*	Canada	Alberta, Northwest Territories	16,895	60.25	-113.25
4	*Dewey Soper Migratory Bird Sanctuary*	Canada	Northwest Territories	8,159	66.17	-74.00
5	*Área de Protección de Flora y Fauna de Términos*	Mexico	Campeche	7,050	18.67	-91.75
6	*Sian Ka"an*	Mexico	Quintana Roo	6,522	19.50	-87.62
7	*Reserva de la Biosfera Archipiélago de Revillagigedo*	Mexico	Mexican Island Territory	6,367	18.83	-112.78
8	*Old Crow Flats*	Canada	Yukon Territory	6,170	67.57	-139.83
9	*Everglades National Park*	United States	Florida	6,105	25.55	-80.92
10	*Río Sabinas*	Mexico	Coahuila de Zaragoza	6,031	27.88	-101.15
South America						
11	*Complejo de humedales del Abanico del río Pastaza*	Peru	Loreto	38,273	-4.00	-75.42
	Pantanal Matogrossense	Brazil	Mato Grosso	1,350	-17.65	-57.42
	Pantanal Boliviano	Bolivia	Santa Cruz	31,899	-18.00	-58.50
12				33,249		
13	*Reentrancias Maranhenses*	Brazil	Maranhão	26,809	-1.68	-45.07
14	*Pacaya Samiria*	Peru	Loreto	20,800	-5.25	-74.67
15	*Baixada Maranhense Environmental Protection Area*	Brazil	Maranhão	17,750	-3.00	-44.95
16	*Los Lípez*	Bolivia	Potosí	14,277	-22.17	-67.40
17	*Lagunas Altoandinas y Puneñas de Catamarca*	Argentina	Catamarca	12,282	-26.87	-67.93
18	*Mamirauá*	Brazil	Amazonas	11,240	-2.30	-66.03
19	*Bañados del Río Dulce y Laguna de Mar Chiquita*	Argentina	Córdoba	9,960	-30.38	-62.77
20	*Lagos Poopó y Uru Uru*	Bolivia	Oruru	9,676	-18.77	-67.12
21	*Lagunas de Guanacache, Desaguadero y del Bebedero*	Argentina	Mendoza, San Juan, San Luis	9,624	-33.00	-67.60
22	*Palmar de las Islas y las Salinas de San José*	Bolivia	Santa Cruz	8,568	-19.25	-61.00
23	*Lago Titicaca (Sector Boliviano)*	Bolivia	La Paz	8,000	-16.17	-68.87

24	*Bañados del Izozog y el río Parapetí*	Bolivia	Santa Cruz	6,159	-18.45	-61.82
25	*Ilha do Bananal*	Brazil	Tocantins	5,623	-10.52	-50.20
26	*Humedales Chaco*	Argentina	Chaco	5,080	-27.33	-58.83
Eurasia						
27	*Réserve Naturelle Nationale des Terres Australes Réserve Naturelle Nationale des Terres Australes Françaises*	France	Terres Australes et Antarctiques Fr.	22,700	-43.12	63.85
28	*Brekhovsky Islands in Ynisei esturay*	Russia	Taimyrsky/Dolgano-Nenets	14,000	70.50	82.75
29	*Tobol-Ishim Forest-steppe*	Russia	Tyumen Oblast	12,170	55.45	69.00
30	*Parapolsky Dol*	Russia	Korak Autonomous Area	12,000	61.62	165.78
31	*Area between the Pura & Mokoritto rivers*	Russia	Taimyrsky/Dolgano-Nenets	11,250	72.53	85.50
32	*Ili River Delta and South Lake Balkhash*	Kazakhstan	Almaty Oblast	9,766	45.60	74.73
33	*Alakol-Sasykkol Lakes System*	Kazakhstan	Almaty, East Kazakhstan Oblasts	9,147	46.27	81.53
34	*Volga Delta*	Russia	Astrakhan Oblast	8,000	45.90	48.78
35	*Dalai Lake National Nature Reserve, Inner Mongolia*	China	Inner Mongolia	7,400	48.55	117.50
36	*Danube Delta*	Romania	Tulcea County	6,470	45.17	29.25
37	*Isyk-Kul State Reserve with the Lake Isyk-Kul*	Kyrgyz		6,236	42.45	77.27
38	*Sundarbans Reserved Forest*	Bangladesh	Khulna	6,017	22.03	89.52
39	*Tonda Wildlife Management Area*	Papua New Guinea	Western Province	5,900	-8.75	141.38
40	*Lake Uvs and its surrounding wetlands*	Mongolia	Uvs Province	5,850	50.33	92.75
41	*Eqalummiut Nunaat and Nassuttuup Nunaa*	Denmark (Greenland)	Kangaatsiaq, Sisimiut	5,795	67.47	-50.82
42	*Runn of Kutch*	Pakistan	Sindh	5,664	24.38	70.08
43	*Lower Dvuobje*	Russia	Khanty-Mansi & Yamalo-Nenets	5,400	64.53	65.77
44	*Aydar Arnasay Lakes System*	Uzbekistan	Dzhizak, Navoi	5,271	40.78	67.77
Africa						
45	*Ngiri-Tumba-Maindombe*	Dem Rep Congo	Equateur, Bandundu	65,696	-1.50	17.50
46	*Grands affluents*	Congo	Plateaux, Cuvette, Sangha, Likouala	59,081	-0.25	16.70
47	*Sudd*	Sudan	Southern Sudan	57,000	7.57	30.65
48	*Okavango Delta System*	Botswana	Ngamiland	55,374	-19.28	22.90
49	*Plaines d‟inondation des Bahr Aouk et Salamat*	Chad	Salamat, Bahr Koh	49,220	10.75	20.55
50	*Delta Intérieur du Niger*	Mali	Mopti, Ségou, Tomboctou	41,195	15.20	-4.10

51	*Malagarasi-Muyovozi Wetlands*	Tanzania	Kigoma, Shinyanga, & Tabora	32,500	-5.00	31.00
52	*Plaines d‟inondation du Logone et les dépressions Toupouri*	Chad	Chari-Baguirmi, Mayo-Kebbi, Tandjilé	29,789	10.50	16.23
	Partie tchadienne du lac Tchad	Chad	Lac, Kenam	16,482	14.33	13.62
	Lake Chad Wetlands in Nigeria	Nigeria	Borno	6,074	13.07	13.80
	Lac Tchad	Niger	Diffa	3,404	14.25	13.33
	Partie Camerounaise du Lac Tchad	Cameroon	Far North Region	1,250	12.77	14.32
53				27,210		
54	*Plaine de Massenya*	Chad	Baguirmi	25,260	11.25	16.25
55	*Gueltas et Oasis de l‟Aïr*	Niger	Agadez	24,132	18.30	9.50
56	*Sangha-Nouabalé-Ndoki*	Congo	Sangha, Likouala	15,250	1.68	16.43
57	*Lake Niassa and its Coastal Zone (Lago Niassa e Zona Costeira)*	Mozambique	Niassa Province	13,637	-12.50	34.85
58	*Banc d‟Arguin*	Mauritania		12,000	20.83	16.75
59	*Suakin-Gulf of Agig*	Sudan	Red Sea State	11,250	18.57	38.08
60	*Bangweulu Swamps*	Zambia	Northern Province	11,000	-11.42	29.98
61	*Dinder National Park (DNP)*	Sudan	Sennar State	10,846	12.32	34.78
62	*Niger-Niandan-Milo*	Guinea	Kankan	10,464	10.50	-9.50
63	*Niger-Mafou*	Guinea	Kankan, Faranah	10,155	9.88	-10.62
64	*Sankarani-Fié*	Guinea	Kankan	10,152	10.42	-8.50
65	*Zambezi Floodplains*	Zambia	Western Province	9,000	-15.25	23.25
66	*Tinkisso*	Guinea	Faranah, Kankan	8,960	11.22	-10.58
67	*Site Ramsar du Complexe W*	Benin	Alibori	8,955	11.83	2.50
68	*Site Ramsar Bas Ogooué*	Gabon	Moyen Ogooué, Ogooué maritime	8,627	-0.65	10.02
69	*Chott Ech Chergui*	Algeria	Saïda	8,555	34.45	0.83
70	*Parc national des Virunga*	Dem Rep Congo	Nord-Kivu	8,000	-1.25	29.50
71	*Kilombero Valley Floodplain*	Tanzania	Morogoro Region	7,967	-8.67	36.17
72	*Le Lac Alaotra: les zones humides et bassins versants*	Madagascar	Ambatondrazaka	7,225	-17.47	48.52
73	*Kafue Flats*	Zambia	Southern & Central Provinces	6,005	-15.68	27.27
74	*Etosha Pan, Lake Oponono & Cuvelai drainage*	Namibia		6,000	-19.25	15.50
75	*The Waza Lagone Floodplain*	Cameroon	Far North Region	6,000	11.63	14.62
76	*Rufiji-Mafia-Kilwa Marine Ramsar Site*	Tanzania	Coast, Lindi Regions	5,969	-8.13	39.63

77	*Zones Humides du Littoral du Togo*	Togo	Maritime	5,910	6.57	1.42
78	*Chott El Jerid*	Tunisia	Tozeur, Kebili	5,862	33.70	8.40
79	*Chott Melghir*	Algeria	El Oued, Biskra, Khenchela	5,515	34.25	6.32
80	*Site Ramsar des Monts Birougou*	Gabon	Ngounié, Ogooué-lolo	5,368	-0.65	10.02
81	*Gambie-Oundou-Liti*	Guinea	Labé	5,274	11.55	-12.30
82	*Bafing-Falémé*	Guinea	Labé	5,173	12.00	-11.50
83	*Conkouati-Douli*	Congo	Kouilou	5,050	-3.92	11.45
Australia						
84	*Coongie Lakes*		South Australia	19,800	-27.45	140.00
85	*Kakadu National Park*		Northern Territory	19,798	-13.02	132.43

Table S3. Simulated global WTD distribution using CLM and Döll-Fiedler recharge.

	% Global Land Area	
WTD Bins (m)	Simulation: CLM Recharge	Simulation: Doll-Fielder Recharge
0	15.7	14.5
0-0.25	2.2	1.8
0.25-1	6.3	5.3
1-2	6.9	5.6
2-3	5.1	5.0
3-5	7.2	7.2
5-10	11.8	11.7
10-20	14.1	13.9
20-40	14.4	14.7
40-100	12.7	15.0
>100	3.6	5.3

Database S1. Water table observations from wells

There are 7 zipped text files organized by continents, with North America separated into 2 files, Canada and US because of the large amount of data.

Africal_obs_wtd.txt.gz (4KB)
Asia_obs_wtd.txt.gz (10KB)
Australia_obs_wtd.txt.gz (674KB)
Canada_obs_wtd.txt.gz (8MB)
Europe_obs_wtd.txt.gz (840KB)
S_America_obs_wtd.txt.gz (321KB)
US_obs_wtd.txt.gz (7MB)

Each text file has 4 columns: latitude, longitude, land elevation (m above sea-level), and water table depth (m below land surface)

Database S2. Model simulated equilibrium water table depth (m below land surface)

There are a 5 zipped NetCDF files for the 5 continents (Asia and Europe combined as Eurasia).

Africa_model_wtd.nc.gz (125MB)
Australia_model_wtd.nc.gz (37MB)
Eurasia_model_wtd.nc.gz (319MB)
N_America_model_wtd.nc.gz (141MB)
S_America_model_wtd.nc.gz (69MB)

Database S3. Fortran90 code of the groundwater flow model as a text file

ewtProgram.f90 (26KB)

Data Access

All data can be downloaded through GLOWASIS, the European Union collaborative project of Global Water Scarcity Information Service, at https://glowasis.deltares.nl/thredds/catalog/opendap/opendap/Equilibrium_Water_Table/catalog.html.

References

1. T. C. Winter, J. W. Harvey, O. L. Franke, W. A. Alley, "Ground water and surface water: A single resource" (USGS Circular 1139, U.S. Government Printing Office, Denver, CO 1998).

2. G. Miguez-Macho, Y. Fan, The role of groundwater in the Amazon water cycle: 1. Influence on seasonal streamflow, flooding and wetlands. *J. Geophys. Res.* **117**, D15113 (2012a). doi:10.1029/2012JD017539

3. Y. Fan, G. Miguez-Macho, A simple hydrologic framework for simulating wetlands in climate and earth system models. *Clim. Dyn.* **37**, 253 (2011). doi:10.1007/s00382-010-0829-8

4. G. Miguez-Macho, Y. Fan, The role of groundwater in the Amazon water cycle: 2. Influence on seasonal soil moisture and evapotranspiration. *J. Geophys. Res.* **117**, (D15), D15114 (2012b). doi:10.1029/2012JD017540

5. D. C. Martre, D. F. Scott, C. Colvin, A review of information on interactions between vegetation and groundwater. *Water S.A.* **25**, 137 (1999).

6. F. Orellana, P. Verma, S. P. Loheide, II, E. Daly, Monitoring and modeling water-vegetation interactions in groundwater-dependent ecosystems. *Rev. Geophys.* **50**, RG3003 (2012). doi:10.1029/2011RG000383

7. D. R. Rossatto, L. de Carvalho Ramos Silva, R. Villalobos-Vega, L. S. L. Sternberg, A. C. Franco, Depth of water uptake in woody plants relates to groundwater level and vegetation structure along a topographic gradient in a neotropical savanna. *Environ. Exp. Bot.* **77**, 259 (2012). doi:10.1016/j.envexpbot.2011.11.025

8. P. Döll, K. Fiedler, Global-scale modeling of groundwater recharge. *Hydrol. Earth Syst. Sci.* **12**, 863 (2008). doi:10.5194/hess-12-863-2008

9. M. Giordano, Global groundwater? Issues and solutions. *Annu. Rev. Environ. Resour.* **34**, 153 (2009). doi:10.1146/annurev.environ.030308.100251

10. T. L. Gleeson *et al*., Mapping permeability over the surface of the Earth. *Geophys. Res. Lett.* **38**, L02401 (2011). doi:10.1029/2010GL045565

11. T. R. Green *et al*., Beneath the surface of global change: Impacts of climate change on groundwater. *J. Hydrol.* **405**, 532 (2011). doi:10.1016/j.jhydrol.2011.05.002

12. A. M. MacDonald, H. C. Bonsor, B. E. O. Docharaigh, R. G. Taylor, Quantitative maps of groundwater resources in Africa. *Environ. Res. Lett.* **7**, 024009 (2012). doi:10.1088/1748-9326/7/2/024009

13. R. G. Taylor *et al*., Ground water and climate change. *Nat. Clim. Change* **3**, nclimate1744 (2012). 10.1038/NCLIMATE1744

14. Materials and methods are available as supplementary material on *Science* Online.

15. H. F. Faure, R. C. Walter, D. R. Grant, The coastal oasis: Ice age springs on emerged continental shelves. *Global Planet. Change* **33**, 47 (2002). doi:10.1016/S0921-8181(02)00060-7

16. B. A. Hawkins *et al*., Energy, water, and broad-scale geographic patterns of species richness. *Ecology* **84**, 3105 (2003). doi:10.1890/03-8006

17. H. Kreft, W. Jetz, Global patterns and determinants of vascular plant diversity. *Proc. Natl. Acad. Sci. U.S.A.* **104**, 5925 (2007). doi:10.1073/pnas.0608361104 Medline

18. E. G. Jobbágy, M. D. Nosetto, P. E. Villagra, R. B. Jackson, Water subsidies from mountains to deserts: Their role in sustaining groundwater-fed oases in a sandy landscape. *Ecol. Appl.* **21**, 678 (2011). doi:10.1890/09-1427.1 Medline

19. B. M. J. Engelbrecht *et al*., Drought sensitivity shapes species distribution patterns in tropical forests. *Nature* **447**, 80 (2007). doi:10.1038/nature05747 Medline

20. C. E. T. Paine, K. E. Harms, J. Ramos, Supplemental irrigation increases seedling performance and diversity in a tropical forest. *J. Trop. Ecol.* **25**, 171 (2009). doi:10.1017/S0266467408005798

21. K. A. Dwire, J. B. Kauffman, J. E. Baham, Plant species distribution in relation to water-table depth and soil redox potential in montane riparian meadows. *Wetlands* **26**, 131 (2006). doi:10.1672/0277-5212(2006)26[131:PSDIRT]2.0.CO;2

22. A. J. Elmore, J. F. Mustard, S. J. Manning, Regional patterns of plant community response to changes in water: Owens Valley, California. *Ecol. Appl.* **13**, 443 (2003). doi:10.1890/1051-0761(2003)013[0443:RPOPCR]2.0.CO;2

23. J. Grogan, J. Galvao, Physiographic and floristic gradients across topography in transitional seasonally dry evergreen forests of southeast Para, Brazil. *Acta Amazon.* **36**, 483 (2006). doi:10.1590/S0044-59672006000400009

24. F. M. R. Hughes, The ecology of African floodplain forests in semi-arid and arid zones: A review. *J. Biogeogr.* **15**, 127 (1988). doi:10.2307/2845053

25. S. Jirka *et al*., Relationships between soil hydrology and forest structure and composition in the southern Brazilian Amazon. *J. Veg. Sci.* **18**, 183 (2007). doi:10.1111/j.1654-1103.2007.tb02529.x

26. R. Pélissier, S. Dray, D. Sabatier, Within-plot relationships between tree species occurrences and hydrological soil constraints: An example in French Guiana investigated through canonical correlation analysis. *Plant Ecol.* **162**, 143 (2002). doi:10.1023/A:1020399603500

27. M. A. Sobrado, Leaf characteristics, wood anatomy and hydraulic properties in tree species from contrasting habitats within upper Rio Negro forests in the Amazon region. *J. Trop. Ecol.* **26**, 215 (2010). doi:10.1017/S0266467409990538

28. J. C. Stromberg, R. Tiller, B. Richter, Effects of groundwater decline on riparian vegetation of semiarid regions: The San Pedro River, Arizona. *Ecol. Appl.* **6**, 113 (1996). doi:10.2307/2269558

29. A. A. Bobrov, D. J. Charman, B. G. Warner, Ecology of testate amoebae (Protozoa: Rhizopoda) on peatlands in western Russia with special attention to niche separation in closely related taxa. *Protist* **150**, 125 (1999). doi:10.1016/S1434-4610(99)70016-7 Medline

30. S. K. Arndt, A. Kahmen, C. Arampatsis, M. Popp, M. Adams, Nitrogen fixation and metabolism by groundwater-dependent perennial plants in a hyperarid desert. *Oecologia* **141**, 385 (2004). doi:10.1007/s00442-004-1655-7 Medline

31. M. R. Bakker, L. Augusto, D. L. Achat, Fine root distribution of trees and understory in mature stands of maritime pine (*Pinus pinaster*) on dry and humid sites. *Plant Soil* **286**, 37 (2006). doi:10.1007/s11104-006-9024-4

32. J. L. Carter, D. A. White, Plasticity in the Huber value contributes to homeostasis in leaf water relations of a mallee Eucalypt with variation to groundwater depth. *Tree Physiol.* **29**, 1407 (2009). doi:10.1093/treephys/tpp076 Medline

33. H. S. Mishra, T. R. Rathore, V. S. Tomar, Root growth, water potential and yield of irrigated wheat. *Irrig. Sci.* **18**, 117 (1999). doi:10.1007/s002710050052

34. J. Stave, G. Oba, A. B. Eriksen, I. Nordal, N. C. Stenseth, Seedling growth of *Acacia tortilis* and *Faidherbia albida* in response to simulated groundwater tables. *For. Ecol. Manage.* **212**, 367 (2005). doi:10.1016/j.foreco.2005.03.023

35. V. L. McGuire, "Water-Level Changes in the High Plains Aquifer, predevelopment to 2007, 2005-06, and 2006-07" (U.S. Geological Survey Scientific Investigations Report 2009-5019, Reston, VA, 2009).

36. N. P. Pellenbarg, "Groundwater Management in the Netherlands: Background and legislation" (Proceedings of ILRI Workshop: Groundwater Management: Sharing Responsibility for an open access resource, Netherlands, 1997).

37. J. J. Cantero, R. Leon, J. M. Cisneros, A. Cantero, Habitat structure and vegetation relationships in central Argentina salt marsh landscapes. *Plant Ecol.* **137**, 79 (1998). doi:10.1023/A:1008071813231

38. J. N. Aranibar *et al*., Nitrate dynamics in the soil and unconfined aquifer in arid groundwater coupled ecosystems of the Monte desert, Argentina. *J. Geophys. Res.* **116**, (G4), G04015 (2011). doi:10.1029/2010JG001618

39. E. Carol, E. Kruse, J. Pousa, Environmental hydrogeology of the southern sector of the Samborombon Bay wetland, Argentina. *Environ. Geol.* **54**, 95 (2008). doi:10.1007/s00254-007-0796-5

40. V. Engel, E. G. Jobbagy, M. Stieglitz, M. Williams, R. B. Jackson, Hydrologic consequences of Eucalyptus afforestation in the Argentine Pampas. *Water Resour. Res.* **41**, W10409 (2005). doi:10.1029/2004WR003761

41. M. G. Garcia, M. V. Hidalgo, M. A. Blesa, Geochemistry of groundwater in the alluvial plain of Tucuman Province, Argentina. *Hydrogeol. J.* **9**, 597 (2001). doi:10.1007/s10040-001-0166-4

42. E. Kruse, J. Ainchil, Fluoride variations in groundwater of an area in Buenos Aires Province, Argentina. *Environ. Geol.* **44**, 86 (2003).

43. O. M. Quiroz Londonñ, D. E. Martinez, C. Dapeña, H. Massone, Hydrogeochemistry and isotope analyses used to determine groundwater recharge and flow in low-gradient catchments of the province of Buenos Aires, Argentina. *Hydrogeol. J.* **16**, 1113 (2008). doi:10.1007/s10040-008-0289-y

44. S. E. Martinez, J. J. Carrillo-Rivera, Socio-economic constraints of groundwater in Capital La Rioja, Argentina. *Environ. Geol.* **49**, 875 (2006). doi:10.1007/s00254-006-0183-7

45. A. Osella, A. Favetto, P. Martinelli, D. Cernadas, Electrical imaging of an alluvial aquifer at the Antinaco-Los Colorados tectonic valley in the Sierras Pampeanas, Argentina. *J. Appl. Geophys.* **41**, 359 (1999). doi:10.1016/S0926-9851(99)00003-8

46. L. B. Rodríguez, P. A. Cello, C. A. Vionnet, Modeling stream-aquifer interactions in a shallow aquifer, Choele Choel Island, Patagonia, Argentina. *Hydrogeol. J.* **14**, 591 (2006). doi:10.1007/s10040-005-0472-3

47. C. Sainato *et al*., Electrical conductivity and depth of groundwater at the Pergamino zone (Buenos Aires Province, Argentina) through vertical electrical soundings and geostatistical analysis. *J. S. Am. Earth Sci.* **16**, 177 (2003). doi:10.1016/S0895-9811(03)00027-0

48. E. D. Schulze *et al*., Rooting depth, water availability, and vegetation cover along an aridity gradient in Patagonia. *Oecologia* **108**, 503 (1996). doi:10.1007/BF00333727

49. P. L. Smedley, B. Nicolli, D. M. J. Macdonald, A. J. Barros, J. O. Tullio, Hydrogeochemistry of arsenic and other inorganic constituents in groundwaters from La Pampa, Argentina. *Appl. Geochem.* **17**, 259 (2002). doi:10.1016/S0883-2927(01)00082-8

50. M. A. Taboada, R. S. Lavado, G. Rubio, D. J. Cosentino, Soil volumetric changes in nitric soils caused by air entrapment following seasonal ponding and water table rise. *Geoderma* **101**, 49 (2001). doi:10.1016/S0016-7061(00)00089-6

51. P. E. Villagra, R. Villalba, J. A. Boninsegna, Structure and growth rate of Prosopis flexuosa woodlands in two contrasting environments of the central Monte desert. *J. Arid Environ.* **60**, 187 (2005). doi:10.1016/j.jaridenv.2004.03.016

52. M. H. Costa *et al*., A macroscale hydrological data set of river flow routing parameters for the Amazon Basin. *J. Geophys. Res.* **107**, (D20), 8039 (2002). doi:10.1029/2000JD000309

53. A. C. Almeida, J. V. Soares, J. J. Landsberg, G. D. Rezende, Growth and water balance of Eucalyptus grandis hybrid plantations in Brazil during a rotation for pump production. *For. Ecol. Manage.* **251**, 10 (2007). doi:10.1016/j.foreco.2007.06.009

54. D. S. S. Babu, A. K. Sahai, M. A. Noernberg, E. Marone, Hydraulic response of a tidally forced coastal aquifer, Pontal do Parana, Brazil. *Hydrogeol. J.* **16**, 1427 (2008). doi:10.1007/s10040-008-0334-x

55. R. Bertolo, R. Hirata, O. Sracek, Geochemistry and geochemical modeling of unsaturated zone in a tropical region in Urania, Sao Paulo state, Brazil. *J. Hydrol. (Amst.)* **329**, 49 (2006). doi:10.1016/j.jhydrol.2006.02.001

56. L. S. Borma *et al*., Atmosphere and hydrologic controls of the evapotranspiration over a floodplain forest in the Bananal Island region, Amazonia. *J. Geophys. Res.* **114**, (G1), G01003 (2009). doi:10.1029/2007JG000641

57. L. Carbo, V. Souza, E. F. G. C. Dores, M. L. Ribeiro, Determination of pesticides multiresidues in shallow groundwater in a cotton-growing region of Mato Grosso, Brazil. *J. Braz. Chem. Soc.* **19**, 1111 (2008). doi:10.1590/S0103-50532008000600009

58. L. A. Cuartas, Thesis, Instituto Nacional de Pesquisas Espaciais, Sao Jose dos Campos (2008).

59. D. C. Garcia-Montiel *et al*., Estimating seasonal changes in volumetric soil water content at landscape scales in a savanna ecosystem using two-dimensional resistivity profiling. *Earth Interact.* **12**, 1 (2008). doi:10.1175/2007EI238.1

60. H. Kreibich, J. Kern, Nitrogen fixation and denitrification in a floodplain forest near Manaus, Brazil. *Hydrol. Processes* **17**, 1431 (2003). doi:10.1002/hyp.1294

61. J. M. de Moraes, A. E. Schuler, T. Dunne, R. D. O. Figueiredo, R. L. Victoria, Water storage and runoff processes in plinthic soils under forest and pasture in eastern Amazonia. *Hydrol. Processes* **20**, 2509 (2006). doi:10.1002/hyp.6213

62. D. Selhorst, S. A. Vieira, I. F. Brown, Água e crescimento de uma floresta na Amazônia Sul-Ocidental, Acre, Brasil: chuva afeta crescimento, mas nível do lençol freático não (ftp://lba.cptec.inpe.br/lba_archives/LC/LC-02/Posters/SelhorstDiogo_Poster_VI_CEB_02nov03.pdf) (Poster presentation, 2002).

63. G. L. Vourlitis *et al*., Energy balance and canopy conductance of a tropical semi-deciduous forest of the southern Amazon Basin. *Water Resour. Res.* **44**, W03412 (2008). doi:10.1029/2006WR005526

64. F. A. Squeo *et al*., Groundwater dynamics in a coastal aquifer in north-central Chile: Implications for groundwater recharge in an arid ecosystem. *J. Arid Environ.* **67**, 240 (2006). doi:10.1016/j.jaridenv.2006.02.012

65. O. Lähteenoja, S. Page, High diversity of tropical peatland ecosystem types in the Pastaza-Marañón basin, Peruvian Amazonia. *J. Geophys. Res.* **116**, (G2), G02025 (2011). doi:10.1029/2010JG001508

66. R. L. H. Poels, *Soils, Water and Nutrients in a Forest Ecosystem in Suriname* (Agric. Univ., Wageningen, The Netherlands, 1987).

67. F. Bongers, D. Engelen, H. Klinge, Phytomass structure of natural plant communities on spodosols in southern Venezuela: the Bana woodland. *Vegetatio* **63**, 13 (1985). doi:10.1007/BF00032183

68. D. A. Coomes, P. J. Grubb, Amazonian caatinga and related communities at La Esmeralda, Venezuela: forest structure, physiognomy and floristics, and control by soil factors. *Vegetatio* **122**, 167 (1996). doi:10.1007/BF00044699

69. A. Guendouz, A. S. Moulla, B. Remini, J. L. Michelot, Hydrochemical and isotopic behaviour of a Saharan phreatic aquifer suffering severe natural and anthropic constraints (case of Oued-Souf region, Algeria). *Hydrogeol. J.* **14**, 955 (2006). doi:10.1007/s10040-005-0020-1

70. B. Kamagate *et al*., Hydrological processes and water balance of a tropical crystalline bedrock catchment in Benin (Donga, upper Ouémé River). *C. R. Geosci.* **339**, 418 (2007).

71. A. Guyot, J.-M. Cohard, S. Anquetin, S. Galle, C. R. Lloyd, Combined analysis of energy and water balances to estimate latent heat flux of a Sudanian small catchment. *J. Hydrol. (Amst.)* **375**, 227 (2009). doi:10.1016/j.jhydrol.2008.12.027

72. M. Le Lay *et al*., Model representation of the Sudanian hydrological processes: Application on the Donga catchment (Benin). *J. Hydrol. (Amst.)* **363**, 32 (2008). doi:10.1016/j.jhydrol.2008.09.006

73. T. S. McCarthy, Groundwater in the wetlands of the Okavango Delta, Botswana, and its contribution to the structure and function of the ecosystem. *J. Hydrol. (Amst.)* **320**, 264 (2006). doi:10.1016/j.jhydrol.2005.07.045

74. L. Ramberg, P. Wolski, M. Krah, Water Balance and Infiltration in a Seasonal Floodplain in the Okavango Delta, Botswana. *Wetlands* **26**, 677 (2006). doi:10.1672/0277-5212(2006)26[677:WBAIIA]2.0.CO;2

75. P. Wolski, H. H. G. Savenije, Dynamics of floodplain-island groundwater flow in the Okavango Delta, Botswana. *J. Hydrol. (Amst.)* **320**, 283 (2006). doi:10.1016/j.jhydrol.2005.07.027

76. E. Temgoua, H.-B. Djeuda Tchapnga, E. Tanawa, C. Guenat, H.-R. Pfeifer, Groundwater fluctuations and footslope ferricrete soils in the humid tropical zone of southern Cameroon. *Hydrol. Processes* **19**, 3097 (2005). doi:10.1002/hyp.5834

77. A. Chouret, P. Mathieu, La nappe phreatique a la peripherie du Lac Tchad: Resultats preliminaires des travaux recents de l'Orstom, 3e Conférence de Géologie Africaine, Khartoum, Soudan, 3–17 Janvier, 1976.

78. S. A. Isiorho, G. Matisoff, K. S. When, Seepage relationships between Lake Chad and the Chad aquifers. *Ground Water* **348**, 19 (1996).

79. R. J. Bowell, P. Foster, A. P. Gize, The mobility of gold in tropical rain forest soils. *Econ. Geol.* **88**, 999 (1993). doi:10.2113/gsecongeo.88.5.999

80. A. A. Shaki, A. J. Adeloye, Evaluation of quantity and quality of irrigation water at Gadowa irrigation project in Murzuq basin, southwest Libya. *Agric. Water Manage.* **84**, 193 (2006). doi:10.1016/j.agwat.2006.01.012

81. E. H. El Idrysy, F. De Smedt, A comparative study of hydraulic conductivity estimations using geostatistics. *Hydrogeol. J.* **15**, 459 (2007). doi:10.1007/s10040-007-0166-0

82. O. Dahan *et al*., Dynamics of flood water infiltration and ground water recharge in hyperarid desert. *Ground Water* **46**, 450 (2008). doi:10.1111/j.1745-6584.2007.00414.x Medline

83. F. Elbaz-Poulichet, G. Favreau, C. Leduc, J.-L. Seidel, Major ion chemistry of groundwaters in the Continental Terminal water table of southwestern Niger (Africa). *Appl. Geochem.* **17**, 1343 (2002). doi:10.1016/S0883-2927(02)00024-0

84. J. Rueedi *et al*., Estimating amount and spatial distribution of groundwater recharge in the Iullemmeden basin (Niger) based on 3H, 3He and CFC-11 measurements. *Hydrol. Processes* **19**, 3285 (2005). doi:10.1002/hyp.5970

85. D. M. Smith, P. G. Jarvis, J. C. W. Odongo, Sources of water used by trees and millet in Sahelian windbreak systems. *J. Hydrol. (Amst.)* **198**, 140 (1997). doi:10.1016/S0022-1694(96)03311-2

86. M. T. Lahai, I. J. Ekanayake, Accumulation and distribution of dry matter in relation to root yield of cassava under a fluctuating water table in inland valley ecology. *Afr. J. Biotechnol.* **8**, 4895 (2009).

87. F. C. Do *et al*., Stable annual pattern of water use by Acacia tortilis in Sahelian Africa. *Tree Physiol.* **28**, 95 (2008). doi:10.1093/treephys/28.1.95 Medline

88. M. E. de Vries *et al*., Rice production with less irrigation water is possible in a Sahelian environment. *Field Crops Res.* **116**, 154 (2010). doi:10.1016/j.fcr.2009.12.006

89. M. T. Lahai, J. B. George, I. J. Ekanayake, Cassava (*Manihot esculenta* Crantz) growth indices, root yield and its components in upland and inland valley ecologies of Sierra Leone. *J. Agron. Crop Sci.* **182**, 239 (1999). doi:10.1046/j.1439-037x.1999.00299.x

90. M. C. Humphries, A. Kindness, W. N. Ellery, J. C. Hughes, Sediment geochemistry, mineral precipitation and clay neoformation on the Mkuze River floodplain, South Africa. *Geoderma* **157**, 15 (2010). doi:10.1016/j.geoderma.2010.03.010

91. L. B. Otter, M. C. Scholes, Methane sources and sinks in a periodically flooded South African savanna. *Global Biogeochem. Cycles* **14**, 97 (2000). doi:10.1029/1999GB900068

92. W. Roets *et al*., Determining discharges from the Table Mountain Group (TMG) aquifer to wetlands in the Southern Cape, South Africa. *Hydrobiologia* **607**, 175 (2008). doi:10.1007/s10750-008-9389-x

93. L. Været, B. Kelbe, S. Haldorsen, R. H. Taylor, A modeling study of the effects of land management and climatic variations on groundwater inflow to Lake St Lucia, South Africa. *Hydrogeol. J.* **17**, 1949 (2009). doi:10.1007/s10040-009-0476-5

94. O. A. E. Abdalla, Aquifer systems in Kordofan, Sudan: Subsurface lithological model. *S. Afr. J. Geol.* **109**, 585 (2006). doi:10.2113/gssajg.109.4.585

95. A. E. M. Elsheikh, K. A. Elsayed Zeielabdein, I. A. A. Babikir, Groundwater balance in the Khor Arbaat basin, Red Sea State, eastern Sudan. *Hydrogeol. J.* **17**, 2075 (2009). doi:10.1007/s10040-009-0541-0

96. A. Guyot, J.-M. Cohard, S. Anquetin, S. Galle, C. R. Lloyd, Combined analysis of energy and water balances to estimate latent heat flux of a Sudanian small catchment. *J. Hydrol. (Amst.)* **375**, 227 (2009). doi:10.1016/j.jhydrol.2008.12.027

97. B. Askri, R. Bouhlila, J. O. Job, Development and application of a conceptual hydrologic model to predict soil salinity within modern Tunisian oases. *J. Hydrol. (Amst.)* **380**, 45 (2010). doi:10.1016/j.jhydrol.2009.10.022

98. I. Chenini, A. B. Mammou, M. M. Turki, E. Mercier, Groundwater resources in Maknassy basin (central Tunisia): Hydrological data analysis and water budgeting. *Geosci. J.* **12**, 385 (2008). doi:10.1007/s12303-008-0038-1

99. A. B. Moussa, S. B. H. Salem, K. Zouari, F. Jlassi, Hydrochemical and isotopic investigation of the groundwater composition of an alluvial aquifer, Cap Bon Peninsula, Tunisia. *Carbonates Evaporites* **25**, 161 (2010). doi:10.1007/s13146-010-0020-7

100. M. Zammouri, Case study of water table evaporation at Ichkeul Marshes (Tunisia). *J. Irrig. Drain. Eng.* **127**, 265 (2001). doi:10.1061/(ASCE)0733-9437(2001)127:5(265)

101. M. Zammouri, H. Feki, Managing releases from small upland reservoirs for downstream recharge in semi-arid basins (Northeast of Tunisia). *J. Hydrol. (Amst.)* **314**, 125 (2005). doi:10.1016/j.jhydrol.2005.03.011

102. R. G. Taylor, K. W. F. Howard, Lithological evidence for the evolution of weathered mantles in Uganda by tectonically controlled cycles of deep weathering and stripping. *Catena* **35**, 65 (1999). doi:10.1016/S0341-8162(98)00118-0

103. M. C. Masiyandima, N. van de Giesen, S. Diatta, P. N. Windmeijer, T. S. Steenhuis, The hydrology of inland valleys in the sub-humid zone of West Africa: Rainfall-runoff processes in the M'bé experimental watershed. *Hydrol. Processes* **17**, 1213 (2003). doi:10.1002/hyp.1191

104. J. A. Butterworth *et al*., Hydrological processes and water resources management in a dryland environment III: Groundwater recharge and recession in a shallow weathered aquifer. *Hydrol. Earth Syst. Sci.* **3**, 345 (1999). doi:10.5194/hess-3-345-1999

105. M. Shamsudduha, R. G. Taylor, K. M. Ahmed, A. Zahid, The impact of intensive groundwater abstraction on recharge to a shallow regional aquifer system: Evidence from Bangladesh. *Hydrogeol. J.* **19**, 901 (2011). doi:10.1007/s10040-011-0723-4

106. M. Shamsudduha, R. G. Taylor, L. Longuevergne, Monitoring groundwater storage changes in the highly seasonal humid tropics: Validation of GRACE measurements in the Bengal Basin. *Water Resour. Res.* **48**, W02508 (2012). doi:10.1029/2011WR010993

107. T. Nobuhiro *et al*., Evapotranspiration during the late rainy season and middle of the dry season in the watershed of an evergreen forest area, central Cambodia. *Hydrol. Processes* **22**, 1281 (2008). doi:10.1002/hyp.6938

108. J. Bai *et al*., Spatial distribution characteristics of organic matter and total nitrogen of marsh soils in river marginal wetlands. *Geoderma* **124**, 181 (2005). doi:10.1016/j.geoderma.2004.04.012

109. B. Chaolun, B. He, R. Gao, L. Wang, Pumping decisions for sustainable development of groundwater resources in areas of grassland degradation: A case study in Lanqi Banner, Inner Mongolia, China. *Hydrogeol. J.* **16**, 1101 (2008). doi:10.1007/s10040-008-0296-z

110. Y. Chen *et al*., Response of riparian vegetation to water-table changes in the lower reaches of Tarim River, Xinjiang Uygur, China. *Hydrogeol. J.* **16**, 1371 (2008). doi:10.1007/s10040-008-0306-1

111. J. S. Chen, C.-Y. Wang, Rising springs along the silk road. *Geology* **37**, 243 (2009). doi:10.1130/G25472A.1

112. B. Cui, Q. Yang, K. Zhang, X. Zhao, Z. You, Responses of saltcedar (*Tamarix chinensis*) to water table depth and soil salinity in the Yellow River Delta, China. *Plant Ecol.* **209**, 279 (2010). doi:10.1007/s11258-010-9723-z

113. D. Han *et al*., A survey of groundwater levels and hydrogeochemistry in irrigated fields in the Karamay Agricultural Development Area, northwest China: Implications for soil and groundwater salinity resulting from surface water transfer for irrigation. *J. Hydrol. (Amst.)* **405**, 217 (2011). doi:10.1016/j.jhydrol.2011.03.052

114. A. Huo, H. Li, M. Hou, C. Qiao, Relations between surface evapotranspiration and water table: A case study based on remote sensing. *African J. Agric. Res.* **6**, 6653 (2011).

115. J. Li, H. Zhan, G. Huang, K. You, Tide-induced airflow in a two-layered coastal land with atmospheric pressure fluctuations. *Adv. Water Resour.* **34**, 649 (2011). doi:10.1016/j.advwatres.2011.02.014

116. D. Y. Liu, W. X. Ding, Z. J. Jia, Z. C. Cai, Relation between methanogenic archaea and methane production potential in selected natural wetland ecosystems across China. *Biogeosciences* **8**, 329 (2011). doi:10.5194/bg-8-329-2011

117. Z. Pang, T. Huang, Y. Chen, Diminished groundwater recharge and circulation relative to degrading riparian vegetation in the middle Tarim River, Xinjiang Uygur, Western China. *Hydrol. Processes* **24**, 147 (2010).

118. J. Qian, H. Zhan, Y. Wu, F. Li, J. Wang, Fractured-karst spring-flow protections: A case study in Jinan, China. *Hydrogeol. J.* **14**, 1192 (2006). doi:10.1007/s10040-006-0061-0

119. I. Säumel, D. Ziche, R. Yu, I. Kowarik, D. Overdieck, Grazing as a driver for *Populus euphratica* woodland degradation in the semi-arid Aibi Hu region, northwestern China. *J. Arid Environ.* **75**, 265 (2011). doi:10.1016/j.jaridenv.2010.10.013

120. C. Song, L. Sun, Y. Huang, Y. Wang, Z. Wan, Carbon exchange in a freshwater marsh in the Sanjiang Plain, northeastern China. *Agric. Meteorol.* **151**, 1131 (2011). doi:10.1016/j.agrformet.2011.04.001

121. Y. Sun, S. Kang, F. Li, L. Zhang, Comparison of interpolation methods for depth to groundwater and its temporal and spatial variations in the Minqin oasis of northwest China. *Environ. Model. Softw.* **24**, 1163 (2009). doi:10.1016/j.envsoft.2009.03.009

122. X. Sun, C. Mu, C. Song, Seasonal and spatial variations of methane emissions from montane wetlands in Northeast China. *Atmos. Environ.* **45**, 1809 (2011). doi:10.1016/j.atmosenv.2011.01.019

123. X. Wang *et al*., Nebkha formation: Implications for reconstructing environmental changes over the past several centuries in the Ala Shan Plateau, China. *Palaeogeogr. Palaeoclimatol. Palaeoecol.* **297**, 697 (2010). doi:10.1016/j.palaeo.2010.09.020

124. P. Wang *et al*., Impacts of environmental flow controls on the water table and groundwater chemistry in the Ejina Delta, northwestern China. *Environ Earth Sci* **64**, 15 (2011). doi:10.1007/s12665-010-0811-0

125. T. Xie, X. Liu, T. Sun, The effects of groundwater table and flood irrigation strategies on soil water and salt dynamics and reed water use in the Yellow River Delta, China. *Ecol. Modell.* **222**, 241 (2011). doi:10.1016/j.ecolmodel.2010.01.012

126. X. J. Xu *et al*., Possible effects of the Three Gorges dam on the transmission of Schistosoma japonicum on the Jiang Han plain, China. *Ann. Trop. Med. Parasitol.* **94**, 333 (2000). Medline

127. J. Yang, B. Li, S. Liu, A large weighing lysimeter for evapotranspiration and soilwater-groundwater exchange studies. *Hydrol. Processes* **14**, 1887 (2000). doi:10.1002/1099-1085(200007)14:10<1887::AID-HYP69>3.0.CO;2-B

128. J. Yang, S. Wan, W. Deng, G. Zhang, Water fluxes at a fluctuating water table and groundwater contributions to wheat water use in the lower Yellow River flood plain, China. *Hydrol. Processes* **21**, 717 (2007). doi:10.1002/hyp.6246

129. X. Zhu, J. Liu, X. Qian, The influence of Zihe Stream on the groundwater resources of the Dawu well field and on the discharge at the Heiwang iron mine, Zibo City area, Shandong Province, China. *Hydrogeol. J.* **7**, 477 (1999). doi:10.1007/s100400050220

130. Y. Zhu *et al*., Simulation of *Populus euphratica* root uptake of groundwater in an arid woodland of the Ejina Basin, China. *Hydrol. Processes* **23**, 2460 (2009). doi:10.1002/hyp.7353

131. R. Andrade, D. Muralidharan, R. Rangarajan, Pulse responses of an unconfined granite aquifer to precipitation: A recharge evaluation through transient water-level fluctuation. *Curr. Sci.* **89**, 677 (2005).

132. R. K. Bajpai, R. P. Tripathi, Evaluation of non-puddling under shallow water tables and alternative tillage methods on soil and crop parameters in a rice-wheat system in Uttar Pradesh. *Soil Tillage Res.* **55**, 99 (2000). doi:10.1016/S0167-1987(00)00111-2

133. S. Behera, M. K. Jha, S. Kar, Dynamics of water flow and fertilizer solute leaching in lateritic soils of Kharagpur region, India. *Agric. Water Manage.* **63**, 77 (2003). doi:10.1016/S0378-3774(03)00175-6

134. Y. Enzel *et al*., High-resolution holocene environmental changes in the Thar desert, northwestern India. *Science* **284**, 125 (1999). doi:10.1126/science.284.5411.125 Medline

135. M. Hirekhan, S. K. Gupta, K. L. Mishra, Application of WaSim to assess performance of a subsurface drainage system under semi-arid monsoon climate. *Agric. Water Manage.* **88**, 224 (2007). doi:10.1016/j.agwat.2006.12.001

136. M. K. Jha, A. Islam, A. P. Mishra, Effective utilization of Chaurs in North Bihar, India. *J. Agric. Eng. Res.* **60**, 237 (1995). doi:10.1006/jaer.1995.1018

137. S. T. G. Raghu Kanth, S. K. Dash, Evaluation of seismic soil-liquefaction at Guwahati city. *Environ. Earth Sci.* **61**, 355 (2010). doi:10.1007/s12665-009-0347-3

138. G. Kar, R. Singh, A. Kumar, Evaluation of post-rainy season crops and response to irrigation in rice (*Oryza sativa*) fallows under shallow water-table of eastern India. *Indian J. Agric. Sci.* **78**, 293 (2008).

139. K. R. Kuma, D. Pande, A. Misra, L. K. Nanda, Playa sediments of the Didwana Lake, Rajasthan: A new environment for surficial-type uranium mineralisation in India. *J. Geol. Soc. India* **77**, 89 (2011). doi:10.1007/s12594-011-0002-y

140. R. K. Majumdar, N. Majumdar, A. L. Mukherjee, Geoelectric investigations in Bakreswar geothermal area, West Bengal, India. *J. Appl. Geophys.* **45**, 187 (2000). doi:10.1016/S0926-9851(00)00028-8

141. M. V. Manjunatha, R. J. Oosterbaan, S. K. Gupta, H. Rajkumar, H. Jansen, Performance of subsurface drains for reclaiming waterlogged saline lands under rolling topography in Tungabhadra irrigation project in India. *Agric. Water Manage.* **69**, 69 (2004). doi:10.1016/j.agwat.2004.01.001

142. J.-C. Maréchal *et al*., Indirect and direct recharges in a tropical forested watershed: Mule Hole, India. *J. Hydrol. (Amst.)* **364**, 272 (2009). doi:10.1016/j.jhydrol.2008.11.006

143. G. G. Moses, S. N. Rao, Strength behavior of naturally cemented marine clay due to changes in groundwater level. *Mar. Georesour. Geotechnol.* **26**, 160 (2008). doi:10.1080/10641190802161185

144. P. C. Nayak, Y. R. S. Rao, K. P. Sudheer, Groundwater level forecasting in a shallow aquifer using artificial neural network approach. *Water Resour. Manage.* **20**, 77 (2006). doi:10.1007/s11269-006-4007-z

145. J. Perrin, S. Ahmed, D. Hunkeler, The effects of geological heterogeneities and piezometric fluctuations on groundwater flow and chemistry in a hard-rock aquifer, southern India. *Hydrogeol. J.* **19**, 1189 (2011). doi:10.1007/s10040-011-0745-y

146. P. Raj, Topographic factor in the groundwater estimations: A case study in typical semi-arid hard rock environments of Andhra Pradesh. *Environ. Monit. Assess.* **178**, 309 (2011). doi:10.1007/s10661-010-1691-1 Medline

147. J. Ram *et al*., Biodrainage potential of Eucalyptus tereticornis for reclamation of shallow water table areas in north-west India. *Agrofor. Syst.* **69**, 147 (2007). doi:10.1007/s10457-006-9026-5

148. R. Rangarajan, N. C. Mondal, V. S. Singh, S. V. Singh, Estimation of natural recharge and its relation with aquifer parameters in and around Tuticorin town, Tamil Nadu, India. *Curr. Sci.* **97**, 217 (2009).

149. G. T. Rao *et al*., Assessment of groundwater contamination from a hazardous dump site in Ranipet, Tamil Nadu, India. *Hydrogeol. J.* **19**, 1587 (2011). doi:10.1007/s10040-011-0771-9

150. D. V. Reddy, P. Nagabhushanam, B. S. Sukhija, A. G. S. Reddy, Understanding hydrological processes in a highly stressed granitic aquifer in southern India. *Hydrol. Processes* **23**, 1282 (2009). doi:10.1002/hyp.7236

151. H. P. Ritzema, T. V. Satyanarayana, S. Raman, J. Boonstra, Subsurface drainage to combat waterlogging and salinity in irrigated lands in India: Lessons learned in farmers' fields. *Agric. Water Manage.* **95**, 179 (2008). doi:10.1016/j.agwat.2007.09.012

152. L. Ruiz *et al*., Water balance modelling in a tropical watershed under deciduous forest (Mule Hole, India): Regolith matric storage buffers the groundwater recharge process. *J. Hydrol. (Amst.)* **380**, 460 (2010). doi:10.1016/j.jhydrol.2009.11.020

153. A. Sarangi, M. Singh, A. K. Bhattacharya, A. K. Singh, Subsurface drainage performance study using SALTMOD and ANN models. *Agric. Water Manage.* **84**, 240 (2006). doi:10.1016/j.agwat.2006.02.009

154. D. P. Sharma, S. K. Gupta, Subsurface drainage for reversing degradation of waterlogged saline lands. *Land Degrad. Develop.* **17**, 605 (2006). doi:10.1002/ldr.737

155. P. Sharma, R. P. Tripathi, S. Singh, Tillage effects on soil physical properties and performance of rice–wheat-cropping system under shallow water table conditions of Tarai, Northern India. *Eur. J. Agron.* **23**, 327 (2005). doi:10.1016/j.eja.2005.01.003

156. M. Singh *et al*., Biophysical and socioeconomic characterization of a water-stressed area and simulating agri-production estimates and land use planning under normal and extreme climatic events: A case study. *Environ. Monit. Assess.* **142**, 97 (2008). doi:10.1007/s10661-007-9911-z Medline

157. P. D. Sreedevi, K. Subrahmanyam, S. Ahmed, Integrated approach for delineating potential zones to explore for groundwater in the Pageru River basin, Cuddapah District, Andhra Pradesh, India. *Hydrogeol. J.* **13**, 534 (2005). doi:10.1007/s10040-004-0375-8

158. C. Sreenivas, C. K. Reddy, Salinity–sodicity relationships of the Kalipatnam drainage pilot area, Godavari western delta, India. *Irrig. Drain.* **57**, 533 (2008). doi:10.1002/ird.385

159. J. M. Stiefel *et al*., Effects of rainwater-harvesting-induced artificial recharge on the groundwater of wells in Rajasthan, India. *Hydrogeol. J.* **17**, 2061 (2009). doi:10.1007/s10040-009-0491-6

160. T. Subramani, N. Rajmohan, L. Elango, Groundwater geochemistry and identification of hydrogeochemical processes in a hard rock region, Southern India. *Environ. Monit. Assess.* **162**, 123 (2010). doi:10.1007/s10661-009-0781-4 Medline

161. N. Sundararajan, S. Sankaran, T. K. Al-Hosni, Vertical electrical sounding (VES) and multi-electrode resistivity in environmental impact assessment studies over some selected lakes: A case study. *Environ. Earth Sci* **65**, 881 (2012). doi:10.1007/s12665-011-1132-7

162. O. P. Toky *et al*., Biodrainage for preventing water logging and concomitant wood yields in arid agro-ecosystems in North-Western India. *J. Sci. Ind. Res.* **70**, 639 (2011).

163. R. P. Tripathi, P. Sharma, S. Singh, Influence of tillage and crop residue on soil physical properties and yields of rice and wheat under shallow water table conditions. *Soil Tillage Res.* **92**, 221 (2007). doi:10.1016/j.still.2006.03.008

164. A. K. Verma, S. K. Gupta, K. K. Singh, H. S. Chauhan, An analytical solution for design of bi-level drainage systems. *Agric. Water Manage.* **37**, 75 (1998). doi:10.1016/S0378-3774(98)00034-1

165. R. Vijay, A. Sharma, S. S. Ramya, A. Gupta, Fluctuation of groundwater in an urban coastal city of India: A GIS-based approach. *Hydrol. Processes* **25**, 1479 (2011). doi:10.1002/hyp.7914

166. F. K. Zaidi, S. Ahmed, B. Dewandel, J.-C. Maréchal, Optimizing a piezometric network in the estimation of the groundwater budget: A case study from a crystalline-rock watershed in southern India. *Hydrogeol. J.* **15**, 1131 (2007). doi:10.1007/s10040-007-0167-z

167. A. Abtahi, F. Khormali, Genesis and morphological characteristics of mollisols formed in a catena under water table influence in southern Iran. *Commun. Soil Sci. Plant Anal.* **32**, 1643 (2001). doi:10.1081/CSS-100104219

168. M. Z. Ahmadi, A field approach to estimation of humid area drainage coefficients. *Agric. Water Manage.* **29**, 101 (1995). doi:10.1016/0378-3774(95)01186-2

169. R. M. Bagher, M. Rasoul, Effect of groundwater table decline on groundwater quality in Sirjan watershed. *Arab. J. Sci. Engr.* **35**, 197 (2010).

170. M. Chitsazan, Y. Akhtari, A GIS-based DRASTIC model for assessing aquifer vulnerability in Kherran Plain, Khuzestan, Iran. *Water Resour. Manage.* **23**, 1137 (2009). doi:10.1007/s11269-008-9319-8

171. M. Dehghani *et al.*, Radar interferometry time series analysis of Mashhad subsidence. *J. Indian Soc. Remote Sens.* **37**, 147 (2009). doi:10.1007/s12524-009-0006-x

172. V. Gholami, Z. Yousefi, H. Z. Rostami, Modeling of ground water salinity on the Caspian southern coasts. *Water Resour. Manage.* **24**, 1415 (2010). doi:10.1007/s11269-009-9506-2

173. H. Karimi, K. Taheri, Hazards and mechanism of sinkholes on Kabudar Ahang and Famenin plains of Hamadan, Iran. *Nat. Hazards* **55**, 481 (2010). doi:10.1007/s11069-010-9541-6

174. V. Nourani, A. A. Mogaddam, A. O. Nadiri, An ANN-based model for spatiotemporal groundwater level forecasting. *Hydrol. Processes* **22**, 5054 (2008). doi:10.1002/hyp.7129

175. V. Nourani, R. G. Ejlali, M. T. Alami, Spatiotemporal groundwater level forecasting in coastal aquifers by hybrid artificial neural network-geostatistics model: A case study. *Environ. Eng. Sci.* **28**, 217 (2011). doi:10.1089/ees.2010.0174

176. J. Almedeij, F. Al-Ruwaih, Periodic behavior of groundwater level fluctuations in residential areas. *J. Hydrol. (Amst.)* **328**, 677 (2006). doi:10.1016/j.jhydrol.2006.01.013

177. Y. Nakashima, H. Zhou, M. Sato, Estimation of groundwater level by GPR in an area with multiple ambiguous reflections. *J. Appl. Geophys.* **47**, 241 (2001). doi:10.1016/S0926-9851(01)00068-4

178. O. A. E. Abdalla, F. O. Suliman, H. Al-Ajmi, T. Al-Hosni, H. Rollinson, Cyanide from gold mining and its effect on groundwater in arid areas, Yanqul mine of Oman. *Environ. Earth Sci.* **60**, 885 (2010). doi:10.1007/s12665-009-0225-z

179. O. A. E. Abdalla, R. Y. Al-Abri, Groundwater recharge in arid areas induced by tropical cyclones: Lessons learned from Gonu 2007 in Sultanate of Oman. *Environ. Earth Sci.* **63**, 229 (2011). doi:10.1007/s12665-010-0688-y

180. M. Ashraf, M. A. Kahlown, A. Ashfaq, Impact of small dams on agriculture and groundwater development: A case study from Pakistan. *Agric. Water Manage.* **92**, 90 (2007). doi:10.1016/j.agwat.2007.05.007

181. V. A. Chudaeva *et al.*, The composition of groundwaters of Murvaviov-Amursky Peninsula, Primorye, Russia. *Indian J. Mar. Sci.* **37**, 193 (2008).

182. J. Heyer, U. Berger, I. L. Kusin, O. N. Yakovlev, Methane emissions from different ecosystem structures of the subarctic tundra in Western Siberia during midsummer and during the thawing period. *Tellus* **54B**, 231 (2002).

183. A. O. Ivanova, S. N. Dedysh, High abundance of planctomycetes in anoxic layers of a *Sphagnum* peat bog. *Microbiology* **75**, 716 (2006). doi:10.1134/S0026261706060154 Medline

184. J. Kurbatova, C. Li, A. Varlagin, X. Xiao, N. Vygodskaya, Modeling carbon dynamics in two adjacent spruce forests with different soil conditions in Russia. *Biogeosciences* **5**, 969 (2008). doi:10.5194/bg-5-969-2008

185. W. J. F. Standring, M. Dowdall, O. Reistad, I. B. Amundsen, Radioactive contamination of groundwater at the Andreeva Bay Shore Technical Base, Northwest Russia. *J. Radioanal. Nucl. Chem.* **279**, 227 (2009). doi:10.1007/s10967-007-7246-4

186. K. Y. Vinnikov, A. Robock, N. A. Speranskaya, C. A. Schlosser, Scales of temporal and spatial variability of midlatitude soil moisture. *J. Geophys. Res.* **101**, (D3), 7163 (1996). doi:10.1029/95JD02753

187. N. N. Vygodskaya *et al*., Climatic control of stand thinning in unmanaged spruce forests of the southern taiga in European Russia. *Tellus* **54B**, 443 (2002).

188. S. A. Aiban, H. I. Al-Abdul Wahhab, O. S. B. Al-Amoudi, H. R. Ahmed, Performance of a stabilized marl base: A case study. *Construct. Build. Mater.* **12**, 329 (1998). doi:10.1016/S0950-0618(98)00023-3

189. M. H. Basyoni, B. A. Mouse, Sediment characteristics, brine chemistry and evolution of Murayr Sabkha, Arabian (Persian) Gulf, Saudi Arabia. *Arab. J. Sci. Engr.* **34**, 95 (2009).

190. M. Makkawi, A. Al-Shuhall, A cost-effective method to map the top of shallow groundwater systems. *Arab Gulf J. Sci. Res.* **25**, 67 (2007).

191. A. U. Sorman, M. J. Abdulrazzak, H. J. Morel-Seytoux, Groundwater recharge estimation from ephemeral streams. Case study: Wadi Tabalah, Saudi Arabia. *Hydrol. Processes* **11**, 1607 (1997). doi:10.1002/(SICI)1099-1085(19971015)11:12<1607::AID-HYP490>3.0.CO;2-Q

192. J.-Y. Lee *et al*., A review of the National Groundwater Monitoring Network in Korea. *Hydrol. Processes* **21**, 907 (2007). doi:10.1002/hyp.6282

193. Y.-C. Park, Y.-J. Jo, J.-Y. Lee, Trends of groundwater data from the Korean National Groundwater Monitoring Stations: Indication of any change? *Geosci. J.* **15**, 105 (2011). doi:10.1007/s12303-011-0006-z

194. A. R. Lawrence, D. C. Gooddy, P. Kanatharana, W. Meesilp, V. Ramnarong, Groundwater evolution beneath Hat Yai, a rapidly developing city in Thailand. *Hydrogeol. J.* **8**, 564 (2000). doi:10.1007/s100400000098

195. M. Tsubo *et al*., Effects of soil clay content on water balance and productivity in rainfed lowland rice ecosystems in northeast Thailand. *Plant Prod. Sci.* **10**, 232 (2007). doi:10.1626/pps.10.232

196. A. Apaydın, Dual impact on the groundwater aquifer in the Kazan Plain (Ankara, Turkey): Sand–gravel mining and over-abstraction. *Environ. Earth Sci* **65**, 241 (2012). doi:10.1007/s12665-011-1087-8

197. C. Koç, The influence of drainage projects on environmental and wetland ecology. *Environ. Prog.* **27**, 353 (2008). doi:10.1002/ep.10296

198. B. Comakli, K. Haliloglu, A. Dasci, C. Mentese, Improvement of yield and botanical composition in meadows: Effects of N fertilization, irrigation on locations having different water table levels. *Rangeland J.* **31**, 361 (2009). doi:10.1071/RJ08017

199. W. E. Sanford, W. W. Wood, Hydrology of the coastal sabkhas of Abu Dhabi, United Arab Emirates. *Hydrogeol. J.* **9**, 358 (2001). doi:10.1007/s100400100137

200. D. Woodward, C. M. Menges, Application of uphole data from petroleum seismic surveys to groundwater investigations, Abu Dhabi (United Arab Emirates). *Geoexplor.* **27**, 193 (1991). doi:10.1016/0016-7142(91)90022-5

201. O. Husson, P. H. Verburg, M. T. Phung, M. E. F. Van Mensvoort, Spatial variability of acid sulphate soils in the Plain of Reeds, Mekong delta, Vietnam. *Geoderma* **97**, 1 (2000). doi:10.1016/S0016-7061(00)00016-1

202. L. Q. Minh, T. P. Tuong, M. E. F. Van Mensvoort, J. Bouma, Soil and water table management effects on aluminum dynamics in an acid sulphate soil in Vietnam. *Agric. Ecosyst. Environ.* **68**, 255 (1998). doi:10.1016/S0167-8809(97)00158-8

203. R. A. Freeze, J. A. Cherry, *Groundwater* (Prentice-Hall, New Jersey, 1979).

204. C. E. Manning, S. E. Ingebritsen, Permeability of the continental crust: Implications of geothermal data and metamorphic systems. *Rev. Geophys.* **37**, 127 (1999). doi:10.1029/1998RG900002

205. M. B. Cardenas, X.-W. Jiang, Groundwater flow, transport, and residence times through topography-driven basins with exponentially decreasing permeability and porosity. *Water Resour. Res.* **46**, W11538 (2010). doi:10.1029/2010WR009370

206. K. J. Beven, M. J. Kirkby, A physically based, variable contributing area model of basin hydrology. *Hydrol. Sci. Bull.* **24**, 43 (1979). doi:10.1080/02626667909491834

207. R. L. Hooke, Toward a uniform theory of clastic sediment yield in fluvial systems. *Geol. Soc. Am. Bull.* **112**, 1778 (2000). doi:10.1130/0016-7606(2000)112<1778:TAUTOC>2.0.CO;2

208. F. E. Nelson, K. M. Hinkel, in *The Physical Geography of North America*, A. R. Orme, Ed. (Oxford Univ. Press, New York, 2002).

209. T. Zhang, R. G. Barry, K. Knowles, J. A. Heginbottom, J. Brown, Statistics and characteristics of permafrost and ground ice distribution in the Northern Hemisphere. *Polar Geography* **23**, 132 (1999). doi:10.1080/10889379909377670

210. N. C. Brandy, *The Nature and Properties of Soils* (Macmillan, New York, 1984).

211. R. B. Clapp, G. M. Hornberger, Empirical equations for some soil hydraulic properties. *Water Resour. Res.* **14**, 601 (1978). doi:10.1029/WR014i004p00601

212. Y. Wada *et al*., Global depletion of groundwater resources. *Geophys. Res. Lett.* **37**, L20402 (2010). doi:10.1029/2010GL044571

213. M. Rodell *et al*., The global land data assimilation system. *Bull. Am. Meteorol. Soc.* **85**, 381 (2004). doi:10.1175/BAMS-85-3-381

214. Y. Fan, G. Miguez-Macho, Potential groundwater contribution to Amazon evapotranspiration. *Hydrol. Earth Syst. Sci.* **14**, 2039 (2010). doi:10.5194/hess-14-2039-2010

215. J. J. de Vries, Dynamics of the interface between streams and groundwater systems in lowland areas, with reference to stream net evolution. *J. Hydrol. (Amst.)* **155**, 39 (1994). doi:10.1016/0022-1694(94)90157-0

216. J. J. de Vries, Seasonal expansion and contraction of stream networks in shallow groundwater system. *J. Hydrol. (Amst.)* **170**, 15 (1995). doi:10.1016/0022-1694(95)02684-H

217. E. Eltahir, P. J.-F. Yeh, On the asymmetric response of aquifer water level to floods and droughts in Illinois. *Water Resour. Res.* **35**, 1199 (1999). doi:10.1029/1998WR900071

218. M. Marani, E. Eltahir, A. Rinaldo, Geomorphic controls on regional base flow. *Water Resour. Res.* **37**, 2619 (2001). doi:10.1029/2000WR000119

219. G. C. Lines, "Hydrology and surface morphology of the Bonneville salt flats and Pilot Valley playa, Utah" (USGS Water Supply Paper 2057, 1979).

220. Y. Fan, C. J. Duffy, D. S. Oliver, Jr., Density-driven groundwater flow in closed desert basins: Field investigations and numerical experiments. *J. Hydrol. (Amst.)* **196**, 139 (1997). doi:10.1016/S0022-1694(96)03292-1

221. Y. Fan, G. Miguez-Macho, C. P. Weaver, R. Walko, A. Robock, Incorporating water table dynamics in climate modeling: 1. Water table observations and the equilibrium water table. *J. Geophys. Res.* **112**, (D10), D10125 (2007). doi:10.1029/2006JD008111

222. G. Miguez-Macho, H. Li, Y. Fan, Simulated water table and soil moisture climatology over North America. *Bull. Am. Meteorol. Soc.* **89**, 663 (2008). doi:10.1175/BAMS-89-5-663

223. T. E. Dahl, "Wetlands losses in the United States 1780's to 1980's" (U.S. Dept. of the Interior, Fish and Wildlife Service, Washington, DC, 1990).

224. T. Stacke, S. Hagemann, Development and evaluation of a global dynamical wetlands extent scheme. *Hydrol. Earth Syst. Sci.* **16**, 2915 (2012). doi:10.5194/hess-16-2915-2012

225. H. J. Schenk, R. B. Jackson, The global biogeography of roots. *Ecol. Monogr.* **72**, 311 (2002). doi:10.1890/0012-9615(2002)072[0311:TGBOR]2.0.CO;2

226. J. Canadell *et al*., Maximum rooting depth of vegetation types at the global scale. *Oecologia* **108**, 583 (1996). doi:10.1007/BF00329030

227. P. Powell, M. Lock, in *The Nile: Sharing a Scarce Resource*, P. Powell, J. A. Allan, Eds. (Cambridge Univ. Press, UK, 1994).

228. E. A. Stanton, The great marshes of the White Nile. *J. Royal African Soc.* **2**, 375 (1903).